Diurnal Cycle of Surface Flows during 2004 NAME and Comparison to Model Reanalysis

PAUL E. CIESIELSKI AND RICHARD H. JOHNSON

Department of Atmospheric Science, Colorado State University, Fort Collins, Colorado

(Manuscript received 22 August 2007, in final form 31 December 2007)

ABSTRACT

During the North American Monsoon Experiment (NAME), an unprecedented surface dataset was collected over the core monsoon region. Observations from 157 surface sites in this region along with twice-daily Quick Scatterometer (QuikSCAT) oceanic winds were quality controlled and processed into a gridded dataset covering the domain (15°–40°N, 90°–120°W) at 1-h, 0.25° resolution for the period from 1 July to 15 August. Using this dataset, the mean, temporal variability, and diurnal characteristics of the monsoon surface flow are documented with detail not previously possible. Being independent of model data over land, these objectively analyzed surface products are compared to similar analyses from a special North American Regional Reanlysis for NAME (NARR_NAME) that was produced for the same period.

Observed surface fields indicate that a robust land–sea breeze circulation is present over most of the Gulf of California (GoC) region in response to the strong diurnal heating of landmasses on both sides of the gulf. Many details of this land–sea breeze circulation are either missing (e.g., the nighttime/early morning land breeze) or poorly represented in the NARR_NAME. Observations from high elevation sites in the Sierra Madre Occidental (SMO) show weak downslope flows ($\sim$0.5 m s^{-1}), near-saturated conditions, and low cloud bases during nighttime hours. These observations are consistent with the notion that high-terrain nocturnal clouds limit radiational cooling and, thus, nocturnal downslope flows as well. Over land, a cool and dry bias is observed in the NARR_NAME surface fields. This dry bias appears to limit the formation of nighttime cloudiness at high elevations, resulting in stronger radiational cooling at night and slope flows in the NARR_NAME that are 2–3 times stronger than observed. In addition, the daytime transition to surface convergence and rising motion over the western slopes of the SMO occurs about 3 h earlier in the NARR_NAME than observed, which indicates the tendency in the reanalyses to initiate the daily convective cycle too early, similar to that observed in operational forecast models over this region.

Following significant rainfall events, increased soil moisture and evapotranspiration due to vegetative green-up result in a smaller diurnal temperature signal over land and weaker slope flows over the SMO. In response to this weaker heating cycle, the magnitude and offshore extent of the land–sea breeze circulation is observed to diminish as the monsoon progresses.

1. Introduction

A dominant feature of the North American monsoon (NAM) is the strong diurnal signal in the flow induced by heating and cooling of the elevated terrain of Mexico and the western United States (Reiter and Tang 1984). Over the core of the NAM, where 60%–80% of the annual rainfall occurs during the boreal summer months (Adams and Comrie 1997; Bordoni et al. 2004), the Sierra Madre Occidental (SMO) dominates the regional geography, focusing the heaviest rainfall along its western slopes. Interacting with the atmosphere on a wide range of horizontal scales, the SMO exerts a strong control on the diurnal cycle of moisture transport, regions of convergence, and ultimately on where convection is initiated (Berbery 2001). While many aspects of this interaction are still uncertain, datasets collected during the North American Monsoon Experiment (NAME) in 2004 are providing the basis for improved observational and modeling studies of the NAM.

During NAME an unprecedented set of surface and upper-air observations was collected over the core monsoon region (Higgins et al. 2006). These datasets present a unique opportunity to describe the detailed

Corresponding author address: Paul E. Ciesielski, Dept. of Atmospheric Science, Colorado State University, Fort Collins, CO 80523.
E-mail: paulc@atmos.colostate.edu

DOI: 10.1175/2008JCLI2206.1

structure of the monsoon system and to compare findings to those produced by various modeling systems. Partially motivated by the need for a reliable lower boundary condition for computing vertical motion, this study uses the NAME surface data to create an objectively analyzed gridded dataset specifically targeted at defining the surface winds and thermodynamic conditions. Hereafter this dataset is referred to as the Colorado State University (CSU) surface analysis. In this paper, the mean, temporal variability, and diurnal characteristics of the CSU surface fields will be examined for the NAME enhanced observing period (EOP) from 1 July to 15 August. It was during this period that the NAME data network had its optimal coverage, and it also coincides with the period for which the special North American Regional Reanalysis (NARR) for NAME was created.

Previous studies involving surface analyses over the NAM domain have focused primarily on describing the low-level conditions over the Gulf of California (GoC) with an emphasis on gulf surge events. Gulf surges, which occur several times in a typical summer season, are northward surges of cool, moist air along the GoC (Hales 1972; Brenner 1974; Douglas and Leal 2003). Notably, these strong surges are able to transport copious amounts of moisture into the southwestern United States, supporting periods of active convection in this region (Higgins et al. 2004). Recent studies have examined the surface characteristics of gulf surges using Quick Scatterometer (QuikSCAT) winds (Bordoni et al. 2004) and high-temporal-resolution surface data from sites deployed along the GoC coast during NAME (Rogers and Johnson 2007). In an earlier study, six automated surface sites were set up at coastal and island locations in the northern GoC from July 1983 to June 1985 to examine fluctuations in near-surface conditions over a range of temporal scales from seasonal to diurnal (Badan-Dangon et al. 1991). Beyond these studies, detailed analyses of NAM surface conditions over the gulf and adjacent land areas are limited. In this study, the CSU surface analysis for the NAME EOP is used to document the evolution of surface conditions as the monsoon progresses over the entire NAME domain (Fig. 1).

In a recent study utilizing ground-based radar, satellite, and rain gauge data, Nesbitt and Gochis (2008) examined how the diurnal cycles of clouds and precipitation were impacted by topography during the NAME EOP. They found that over the higher terrain of the SMO, shallow, nonprecipitating stratus existed during the overnight hours, developing into shallow convection by noon the following day. They hypothesized that the presence of this nighttime cloud cover over the higher terrain limits radiational cooling and subsequent cooling-induced downslope flows. Such a scenario, if true, has important implications for the initiation of convection later in the day. Because of the location of several surface sites near the ridgetop and west slopes of the SMO (see Fig. 1), a detailed surface analysis in this region allows us to examine the plausibility of these ideas (section 4).

Utilizing the unprecedented set of observations collected during the 2004 NAM, a special version of the NARR was produced (Mo et al. 2007) for the NAME EOP. In this study the special NARR for NAME is referred to as NARR_NAME to distinguish it from the operational version of the NARR. A second goal of this study is to examine the extent to which NARR_NAME products can reproduce these observed surface features. Such a comparison is meaningful in that the CSU gridded analyses are essentially independent of model data[1] and, thus, are not influenced by model parameterizations or other model properties. Such intercomparisons can be utilized to reveal deficiencies in the NARR model physics and assimilation schemes, which hopefully will provide a pathway to model improvements and ultimately better forecasts.

The remainder of this paper is organized as follows. In section 2 the data sources for the CSU surface analysis are discussed along with a description of the analysis procedure, the NARR_NAME, and other data sources for this study. Section 3 examines the EOP-mean fields and differences between the CSU and NARR_NAME analyses. The diurnal cycle of the surface fields is considered in section 4, and its evolution as the monsoon evolves is discussed in section 5. In section 6, observed surface fluxes at two locations (one over the GoC and one inland) are compared to each other and to fluxes from the NARR_NAME. Conclusions and final remarks are offered in section 7.

2. Data and analysis procedures

a. Surface network

The NAME surface observational network is shown in Fig. 1 along with the topography of this region. These surface sites are located at elevations ranging from sea level to nearly 2400 m. Elevations in the SMO typically

[1] The primary use of NARR_NAME data in the CSU analysis is over data-sparse oceanic regions. Sensitivity tests show that the inclusion of model data over the open oceans has little to no impact on analyses over land.

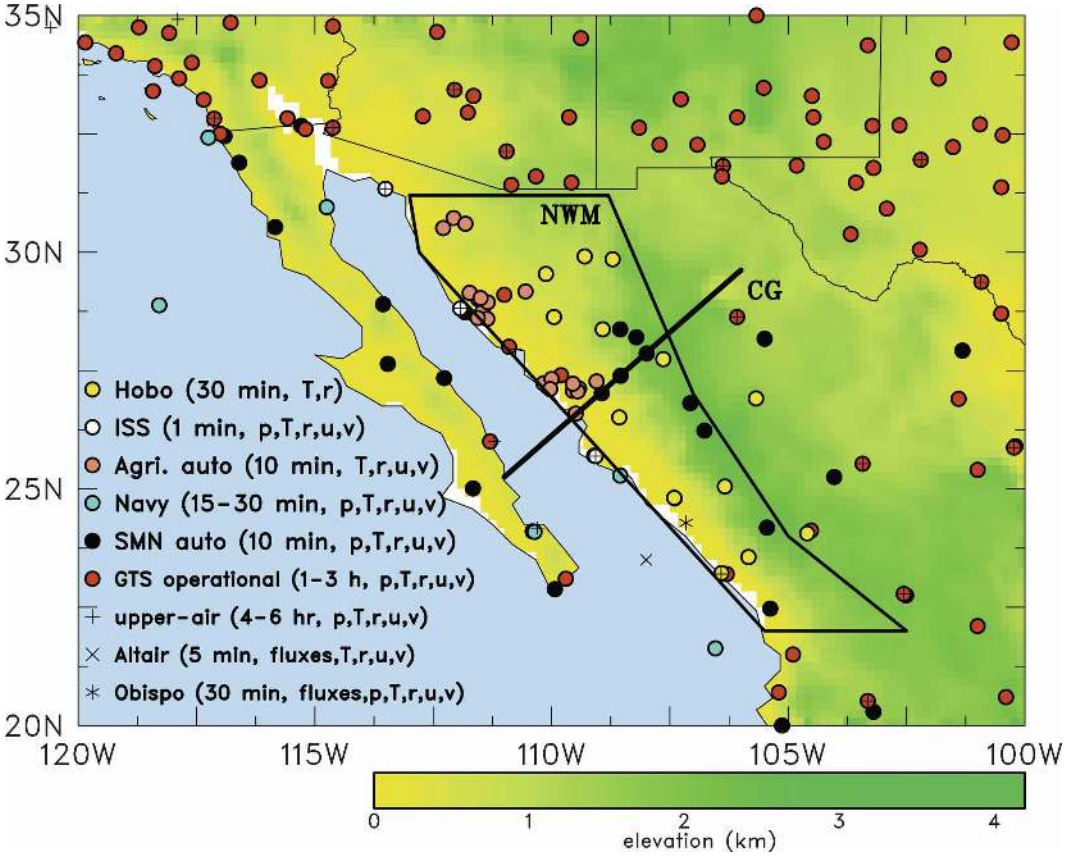

FIG. 1. Surface network during the NAME EOP. Color coding of circles indicates type of site, its temporal resolution, and surface fields observed (where p is pressure, T temperature, r water vapor mixing ratio, u zonal wind component, and v meridional wind component). Line indicates location of cross-gulf (CG) transect for results presented in Figs. 11–14. Polygon shows region over northwestern Mexico (NWM) in which fields were averaged for Figs. 16–18.

exceed 1500 m with several locations rising to over 3000 m. The color coding of the circles in Fig. 1 denotes the origin of the observations, their temporal frequency, and the variables that were observed. Temperature (T) and relative humidity (RH) data at 30-min resolution were obtained from a series of 13 Hobo event recorders, which were collocated with tipping-bucket rain gauges. The remaining sites shown here recorded surface winds in addition to the thermodynamic fields. Several of these sites used automated sensors that recorded data at a high temporal frequency (1–30 min) including the three Integrated Sounding System (ISS) sites supported by the National Center for Atmospheric Research (NCAR), two sites that also measured surface fluxes (Obispo, Sinaloa, and the R/V *Altair* stationed at the mouth of the GoC), nine coastal or island sites supported by the Mexican navy, 25 sites operated by the Mexican Weather Service (Servicio Meteorológico Nacional or SMN), and 23 Sonoran agricultural sites. The surface network also included data from several operational sites (27 in Mexico and 56 in the United States) in which the 1–3-h temporal resolution data were received via the Global Telecommunication System (GTS). Many of the Mexican operational sites did not take nighttime observations. The actual moisture variable analyzed was water vapor mixing ratio, r, which is obtained by converting relative humidity at the given surface temperature and pressure. At the sites with no recorded pressure information (the Hobo and agricultural automated sites), this field was estimated by interpolating the NARR_NAME surface pressure in space and time. In addition, the surface data point from the upper-air soundings was used in the absence of other surface data. Additional information on the data from any of these sources can be obtained from the NAME data catalog, maintained by the Earth Observing Laboratory (EOL) (information online at http://data.eol.ucar.edu/master_list/?project=NAME).

Data from this network, consisting of 157 surface sites, were collected for the 46-day period from 1 July to 15 August 2004. Since each of the above data sources had its own format, the data were first put into a common format, then averaged into hourly bins centered on the hour. Quality control (QC) procedures included application of gross limit checks in which data values that were more than four standard deviations from their 46-day mean were regarded as questionable and not used. Next, time series plots of surface fields for sites in close proximity to each other were visually compared, and obvious outliers were removed. This latter subjective check resulted in the rejection of winds at two sites in Mexico (Don Enrique, Sonora; Presa Emili, Baja). The winds at these sites were either grossly in error or were impacted strongly by local topographic effects. Operational surface data from sites outside the region shown in Fig. 1 (primarily over the United States) were also used in the objective analysis described below. Gross limit checks were applied to these additional data: however, due to the data's immense volume and remoteness to the core monsoon region, the subjective QC procedures described above were not applied to data from these later sites.

b. Other data sources

To supplement the surface wind analysis, 25-km horizontal resolution surface winds over the oceans and GoC, obtained from National Aeronautics and Space Administration's Quick Scatterometer (QuikSCAT), were used (Liu 2002). These winds with overpass times near 0000 and 1200 UTC were available at any given oceanic location in the NAME region ~70% of the time. Missing data were due to swath gaps in the satellite coverage and nonutilization of rain-flagged wind estimates, which tend to be less accurate. Aside from QuikSCAT winds, the R/V *Altair,* stationed at the mouth of the GoC (23.5°N, 108°W) for ~32 days during the NAME EOP, was the only source of surface data over the GoC during this period. This site collected routine surface variables, excluding pressure, but including surface fluxes at 5-min resolution (Zuidema et al. 2007).

As an alternative to merely interpolating the thermodynamic fields across the GoC based on coastal observations, we chose to estimate these fields over the GoC based on SST data and information collected at the *Altair*. The SST dataset used here is the special multiplatform merged (MPM) SST analysis produced by Wang and Xie (2007) and available at 3-h, 0.25° horizontal resolution. While some buoy and ship observations were utilized in generating the MPM SST analysis, no data from the *Altair* were used (C. Huang 2007, personal communication). The EOP-averaged MPM SST field over the GoC (Fig. 2) shows a very warm GoC with the highest temperatures near the mouth of the gulf and along its east side. The cool patch in the northern GoC has been attributed to tidal mixing (Lavín and Organista 1988; Paden et al. 1991; Argote et al. 1995) and is likely related to a cyclonic gyre observed over this region of the gulf in summer (Lavín et al. 1997). The SST diurnal cycle plot in Fig. 2 shows that the MPM analysis interpolated to the *Altair* position compares quite favorably to the independent SST measured at the ship, giving us confidence in this SST analysis. Using the MPM SSTs and the CSU sea level pressure analysis, the saturated water vapor mixing ratio at the ocean surface (r_{sat}) was computed. We then subtracted the mean diurnal cycle difference of SST $- T_s$ and $r_{\text{sat}} - r_s$ (where T_s and r_s are the surface air temperature and water vapor mixing ratio) computed from *Altair* observations (not shown) from the MPM SST and r_{sat} analysis to estimate a T_s and r_s on a 3-h basis. This procedure, which was applied only over the GoC (north of 23°N), assumes that the near-surface gradients of T and r observed at the *Altair* are representative of the entire GoC. A ramification of this assumption is considered in section 3.

The inset plots in Fig. 2 show the diurnal cycle of T_s and r_s measured at the *Altair* (red curves), NARR_NAME values interpolated to the *Altair* position (green curves), and estimated values based on the procedure described above (black curves). Examination of these curves shows that the estimated T_s reproduces well the diurnal cycle at the *Altair*, while the estimated r_s is about 0.5 g kg^{-1} too high compared to the *Altair* observations. On the other hand, the NARR_NAME surface fields have a slight cool (~1°C) and near-zero moisture bias compared to those at the *Altair*. The impact of this cool bias will be discussed further in section 6 when surface fluxes are considered.

The NARR_NAME products used in this study are from a special reanalysis for the NAME EOP. This reanalysis, which used the National Centers for Environmental Prediction (NCEP) Regional Climate Data Assimilation System (RCDAS) (Mesinger et al. 2006), is at 32 km, 45 vertical layers, and 3-h resolution. In addition to the usual data products assimilated into the RCDAS (Mo et al. 2007), this special reanalysis used sounding data from the NAME-enhanced upper-air network (shown in Fig. 1 of Johnson et al. 2007), the MPM SST analysis described above, and an enhanced 3-h precipitation dataset, which is converted into latent heating (Lin et al. 1999). Over land, the assimilated

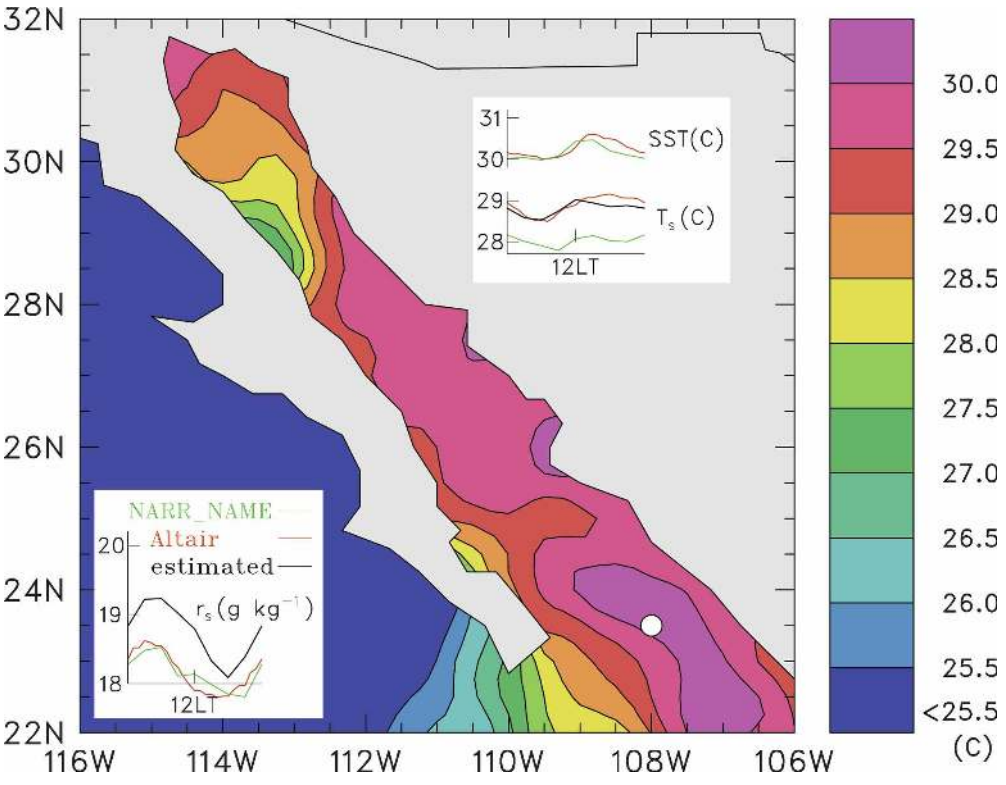

FIG. 2. MPM EOP-mean SST map. Inset plot at lower left shows the diurnal cycle of r_s at the *Altair* (red curve), from the NARR_NAME (green curve), and estimated (as described in the text; black curve) at the *Altair* location (shown by white circle). In a similar fashion, the inset plot at upper right shows the diurnal cycle of T_s at the *Altair* location from these three sources, as well as the diurnal cycle of SST from the *Altair* (red curve) and from the MPM analysis (which is used in the NARR_NAME; green curve).

rainfall data is based on combined daily gauge data (Higgins et al. 2000) and the NAME Event Rain Gauge Network (NERN) (Gochis et al. 2007), located in the core of the monsoon region; over water, Climate Prediction Center (CPC) morphing technique (CMORPH) rainfall data (Joyce et al. 2004) is used. To get 3-h precipitation estimates, hourly precipitation data available from the National Climate Data Center (NCDC) were used to disaggregate the daily data (K. Mo 2007, personal communication). At the surface over land, RCDAS assimilates 10-m winds and 2-m moisture from surface observing systems, but does not assimilate surface temperature (Mesinger et al. 2006). Over the seas, QuikSCAT winds were not assimilated. From Fig. 2 of Mo et al. (2007), it appears that data from ~50 surface sites over the NAME Tier 1 Array (T1A) were used in producing the NARR_NAME, which is about one-third of the number of sites used in the CSU surface analysis.

Precipitation data used in this study are based on the Tropical Rainfall Measuring Mission (TRMM) 3B42v6 algorithm (Huffman et al. 2007). Estimates from this satellite-based dataset, available at 3-h and 0.25° resolution, were shown to compare favorably with ground-based gauge estimates over the NAME region (Johnson et al. 2007; Nesbitt and Gochis 2008).

c. CSU surface analyses and computation of surface vertical motion

Gridded fields of surface variables were analyzed at 1-h, 0.25° horizontal resolution over the NAME Tier 2 domain (15°–40°N, 90°–120°W) for the NAME EOP from 1 July to 15 August using a reciprocal multiquadric interpolation scheme, which is a slight variant of the scheme described in Nuss and Titley (1994). The multiquadric scheme used here has two tuneable parameters: c, which determines the curvature of the interpolating function and controls the strength of gradients that can be resolved, and λ, which sets the amount of smoothing of unresolvable scales. To resolve the large spatial gradients of the surface fields in the vicinity of the GoC, the Gaussian-shaped multiquadric basis function was chosen to have a half-width of 1° (i.e., $c = 0.5$), while λ, the smoothing parameter, was set to 5×10^{-5}. This choice of parameters represents a compromise be-

tween a noisy-looking analysis in which the observations are made to fit exactly and an analysis in which smoothing is used to reduce sampling errors and local-scale features.

The surface fields in the CSU analysis include the zonal and meridional wind components (u_s and v_s, respectively), temperature (T_s), water vapor mixing ratio (r_s), pressure (p_s), and sea level pressure (p_{SL}). This analysis used the quality controlled hourly surface data from sites shown in Fig. 1 along with GTS operational surface data from sites outside the domain shown in this figure. Over the oceans and GoC, QuikSCAT data were used at 0000 and 1200 UTC, and to aid the analysis over the GoC, thermodynamic fields estimated from the SST analysis, as described above, were used. Owing to the lack of data over the oceans, grid points at 0.5° intersections having no surface data within a 0.4° radius were assigned values from NARR_NAME (Mo et al. 2007) surface fields. However, no reanalysis fields were used over land or the GoC. Since the GoC estimated thermodynamic and NARR_NAME fields were available at 3-h resolution, the closest observation times for these analyses were used in generating the 1-h gridded fields.

As in Luo and Yanai (1983), objectively analyzed surface winds were used to calculate the orographically forced vertical motion at the surface by

$$\omega_s = -g\rho_s\left[\left(\frac{u_s}{a\cos\phi}\frac{\partial h}{\partial \lambda} + \frac{v_s}{a}\frac{\partial h}{\partial \phi}\right)\right], \quad (1)$$

where g is gravity, $\rho_s = p_s/RT_s$ the density of the surface air, R the gas constant of dry air, T_s the surface temperature, and h the smoothed terrain height. Values of terrain height were taken from the National Center of Atmospheric Research (NCAR) ⅙°-resolution U.S. Navy elevation dataset. Using unsmoothed terrain heights results in unrealistic surface vertical motions due to the small-scale roughness in the topographic maps. Following the filtering procedure presented in Sardeshmukh and Hoskins (1984), the elevation data were smoothed by creating a high-wavenumber (T485) spectral representation of the topography, truncating it at T213 (~100 km in physical space), and filtering the spectral coefficients with a hyperdiffusive filter of the form

$$\exp\left[-\left(\frac{n(n+1)}{N(N+1)}\right)^2\tau\right], \quad (2)$$

where n is the total wavenumber, $N = 213$, and τ, the reduction factor for the highest wavenumber, was set to reduce its amplitude by 90%. This results in an isotropic smoothing of topography in physical space.

3. Mean surface fields during NAME

While surface analyses were computed over the large-scale Tier 2 NAME domain, this paper focuses on results for the more regional scale T1A domain (20°–35°N, 100°–116°W), which represents the core monsoon region and the area over which the surface observations were subjected to the more stringent quality controls.

Figure 3 shows EOP-mean maps for surface temperature and water vapor mixing ratio from the CSU analysis, the NARR_NAME, and their difference. Both analyses show the same general patterns with hot and dry conditions over the desert Southwest, warm and moist conditions over the GoC and adjacent coastal plains, and cool and drier conditions over the SMO. While both products have similar horizontal resolutions (~30 km), the CSU analysis is characterized by less prominent small-scale features and weaker spatial gradients due to the smoothing properties of its objective analysis scheme.

Several features in the difference fields (rightmost panels in Fig. 3) are worth noting. Since the NARR_NAME is the primary data source for T_s and r_s over the oceans in the CSU analysis, little difference is seen there. Over land, the NARR_NAME analysis tends to be cooler and drier than the CSU. These tendencies are consistent with the biases seen between analyses and observations at individual sites (Fig. 4 and Table 2, which shows the domain average biases). As seen here, the temperature and moisture biases are generally small in the CSU analysis (i.e., predominately yellow shades), whereas the NARR_NAME's cool and dry biases are especially prominent over the SMO and southeast portion of the domain (Figs. 3 and 4). While a complete understanding of the causes for these NARR_NAME biases is beyond the scope of this study, one should recall that the NARR_NAME did not assimilate observed surface temperatures and that it used data from only ~50 surface sites over the T1A domain compared to 157 sites in the CSU analysis.

In contrast to the land areas, over the northern GoC the NARR_NAME is warmer and moister than in the CSU analysis. Since no surface temperature and moisture measurements exist over this region, it is not possible to determine with certainty which analysis is performing better. However, since the NARR_NAME fields validate reasonably well with *Altair* observations as seen in Fig. 2, one might assume that the differences over the northern GoC arise predominantly from biases in the CSU analysis, which was constructed in an ad hoc fashion using the MPM SST analyses and observations of near-surface gradients from the *Altair* (as described

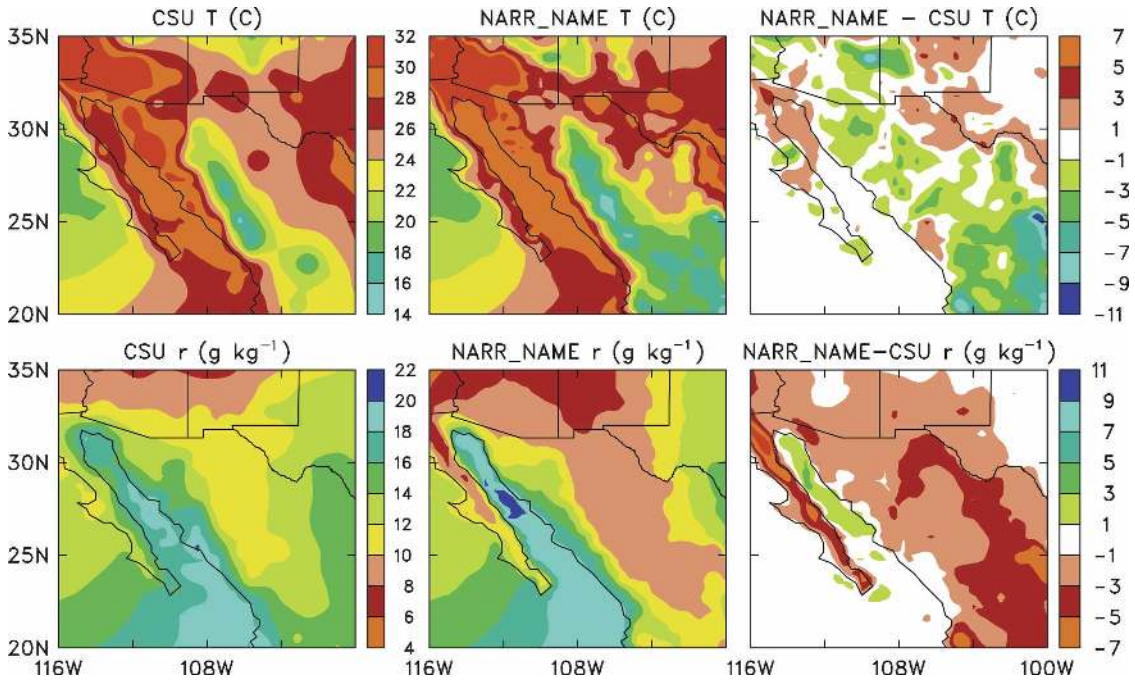

FIG. 3. (top row) EOP-mean surface temperature and (bottom row) water vapor mixing ratio maps based on 3-hourly analyses. (left) CSU analyses, (middle) NARR_NAME, and (right) NARR_NAME − CSU difference. The scales for the CSU and NARR_NAME maps are located between the panels, and the scales for the difference maps are located to their right.

in section 2). Assuming the cool, dry biases in the CSU fields over the northern GoC are real suggests that the actual near-surface vertical gradients of temperature and moisture in this region are, in fact, smaller than those observed farther south at the *Altair*. This is consistent with the notion that prevailing southeasterlies over the GoC advect warm, moist air from the southern GoC over the cooler waters of the northern GoC, resulting in smaller near-surface gradients there.

A comparison of the CSU and NARR_NAME wind analyses is shown in Fig. 5 with the panels from top to bottom showing EOP-mean wind vectors, mean wind speed, and wind persistence, respectively. Here wind persistence, which measures the steadiness of the wind, is defined as the speed of the resultant wind divided by the mean wind speed. While differences over the ocean are again small, the slightly weaker wind speeds off the west coast of Baja in the CSU analysis arise from use of QuikSCAT winds at 0000 and 1200 UTC. Similarly, NARR_NAME winds are almost everywhere stronger as seen in the top panels of Fig. 5 (e.g., stronger westerlies across Baja, stronger southeasterlies in the GoC, stronger westerlies across southern Arizona and northwestern Mexico, and stronger easterlies over much of the eastern portion of the T1A domain). These stronger mean-vector winds in the NARR_NAME are the result of both stronger NARR_NAME wind speeds and higher persistence.

Wind analysis differences are particularly large over the northern GoC (with NARR_NAME wind speeds up to 4.5 m s^{-1} stronger than CSU's) and gradually diminish toward the mouth of the GoC. However, if only 0600 and 1800 LT (where LT = UTC −6 h) times are considered (when QuikSCAT winds are generally present), the difference is 2–3 m s^{-1}, as seen in Fig. 6, which depicts the diurnal cycle of winds for a point over the northern gulf. Also seen here is the poor temporal continuity in the CSU winds over the GoC, which results from interspersing twice-daily QuikSCAT winds with those interpolated from coastal sites. At times when no QuikSCAT winds are available over the GoC, the CSU analysis scheme produces a low wind speed bias by interpolating winds across the gulf from coastal sites, which are characterized by flows that frequently are in opposite directions due to land–sea breeze circulations. While the CSU-analyzed wind speeds in GoC have a low bias, on the other hand, the RCDAS used in the NARR_NAME has been consistently shown to produce a GoC low-level jet that is too strong (Mo et al. 2007). The 2–3 m s^{-1} difference between the analyses at 0600 and 1800 LT in Fig. 6 presumably reflects this high speed bias in the NARR_NAME. The along-gulf EOP-

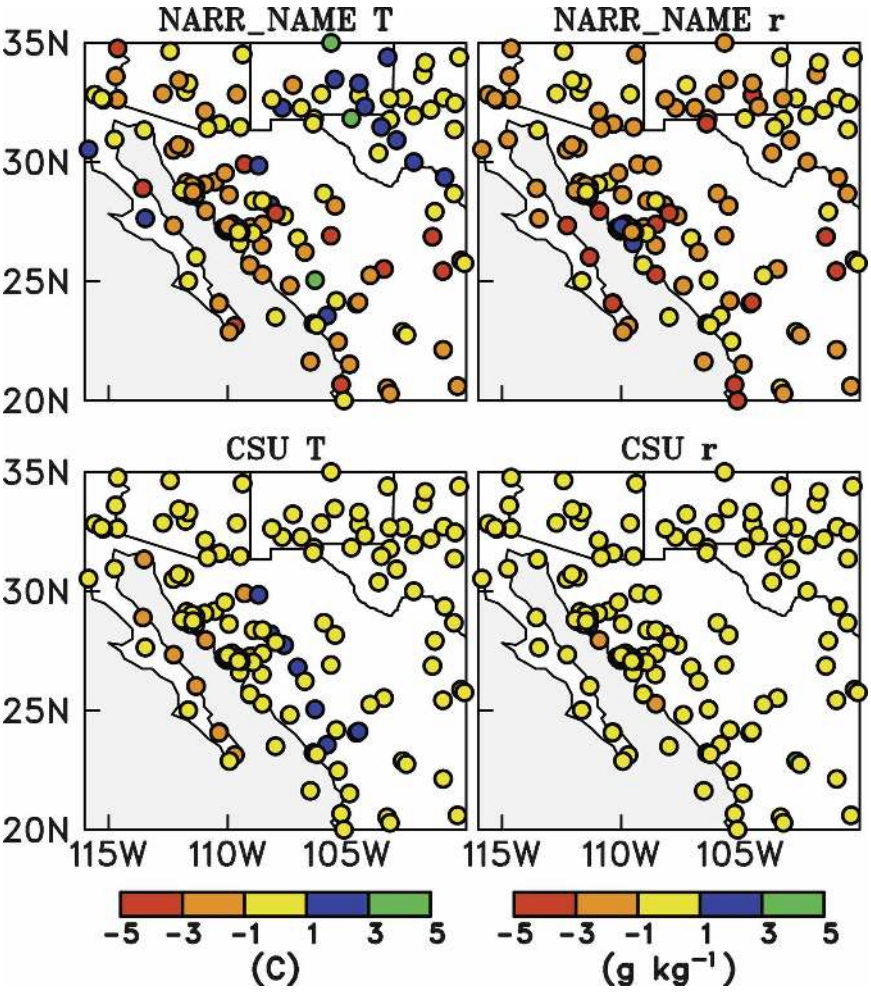

FIG. 4. (left) Surface temperature and (right) moisture biases (analysis − observations) during the NAME EOP at individual surface sites for the (top) NARR_NAME and (bottom) CSU analyses. Warm shades indicate negative biases, cool shades positive biases, and the yellow shade indicates biases around zero.

mean surface pressure difference (computed as the Mazatlan minus Yuma surface pressure) is 26% greater in the NARR_NAME dataset[2] than observed, which could contribute to the excessive NARR_NAME wind speeds in the GoC. Outside the GoC, NARR_NAME wind speeds are larger than CSU's, except over parts of Texas. Based on the smaller RMS errors and biases in the CSU wind components (see Tables 1 and 2), it appears that the CSU analysis, at least over land, is more accurately capturing the monsoonal wind fields.

The wind persistence maps (bottom panels in Fig. 5) are characterized in both analyses by low values along the crest of the SMO where winds are typically light and variable. Differences in persistence are evident elsewhere, but are particularly large along the east coast of Baja and over portions of northwestern Mexico and southwestern Arizona. As will be discussed in the next section, these regions exhibit prominent diurnal wind shifts, which the CSU analysis was able to resolve but are not present in the NARR_NAME.

4. Diurnal cycle of surface fields

In this section the diurnal cycles of surface fields during the NAME EOP are examined using the observed and gridded datasets. While precipitation over the NAME domain has an important modulating influence on surface fields and vegetation (Douglas et al. 2006;

[2] The larger along-gulf pressure gradient in the NARR_NAME is due to higher surface pressures over the southern GoC in the NARR_NAME than observed.

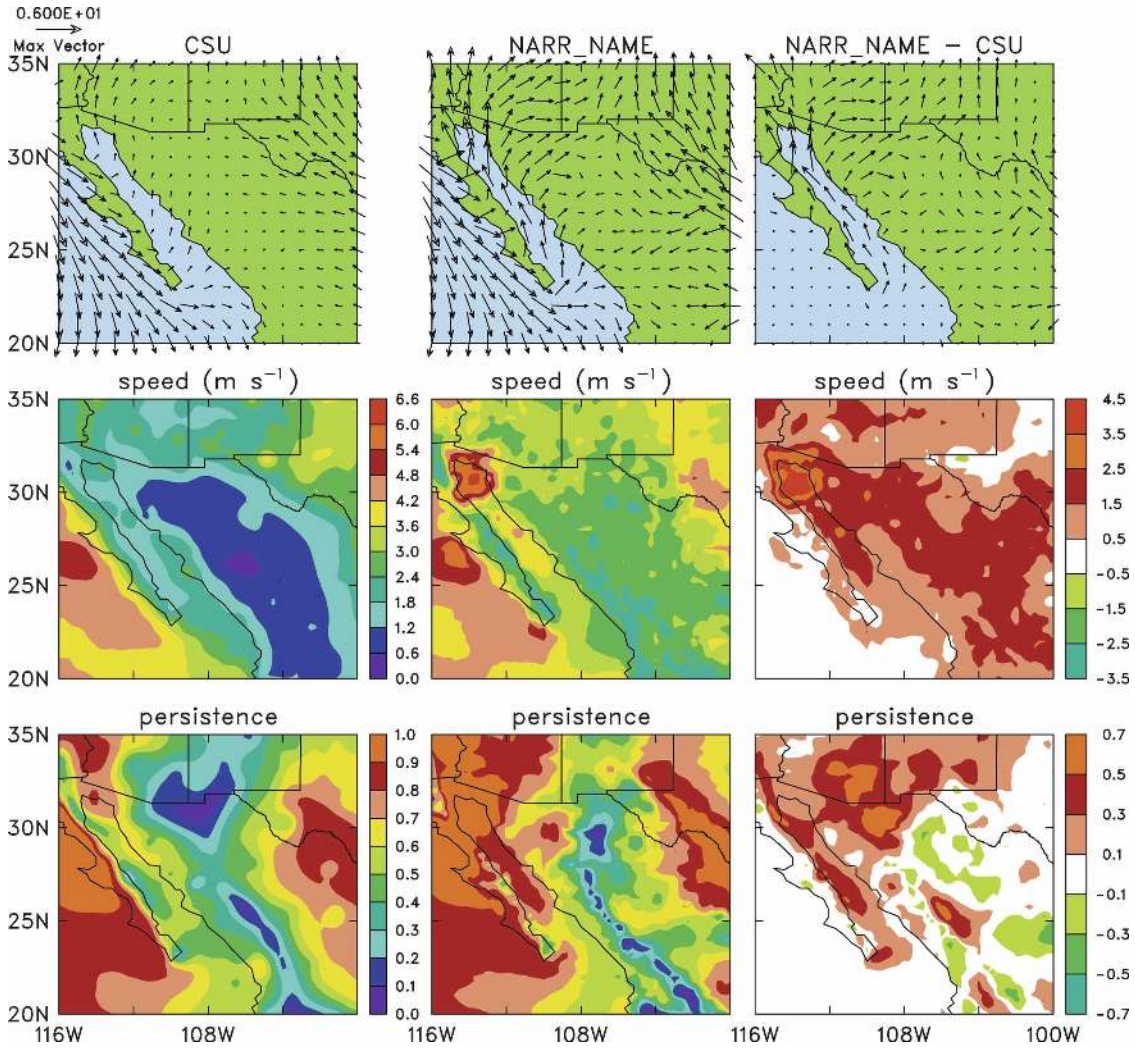

FIG. 5. EOP-mean surface wind analyses: (top row) resultant wind vectors, (middle row) wind speed, and (bottom row) wind persistence maps based on 3-hourly analyses. (left) CSU analyses, (middle) NARR_NAME, and (right) NARR_NAME − CSU difference. The scales for the CSU and NARR_NAME maps are located between the panels, and the scales for the difference maps are located to their right.

Watts et al. 2007—to be considered further in the next section), its diurnal cycle has been the subject of several recent studies (e.g., Gochis et al. 2007; Janowiak et al. 2007; Nesbitt and Gochis 2008) and thus is not considered here.

The diurnal cycle of surface winds at several sites is shown in Fig. 7 with diagrams that depict 3-h-averaged wind vectors. Along the south and east coast of Baja and west coast of the Mexican mainland a prominent land–sea breeze circulation, driven by differential heating between land and sea (Badan-Dangon et al. 1991), is observed. The strength and orientation of this circulation feature vary considerably from site to site, presumably depending on the site's proximity to inland topographic features. The westerly sea-breeze winds along the western Mexican coast diminish inland, with weak winds at the higher elevations of the SMO, especially at night (see Fig. 10, bottom, which compares observed and NARR_NAME winds for seven high elevation locations). At coastal sites over the far northern GoC, nighttime cooling of the land is insufficient to overcome the pressure gradient into the desert heat low and develop a nighttime land breeze. At these sites, a clockwise turning of the winds due to inertial effects is superimposed upon a mean south to southeasterly flow. While early morning (0300–0900 LT) surface winds are relatively weak at northern GoC coastal sites, the low-level southerly jet over this region maximizes at

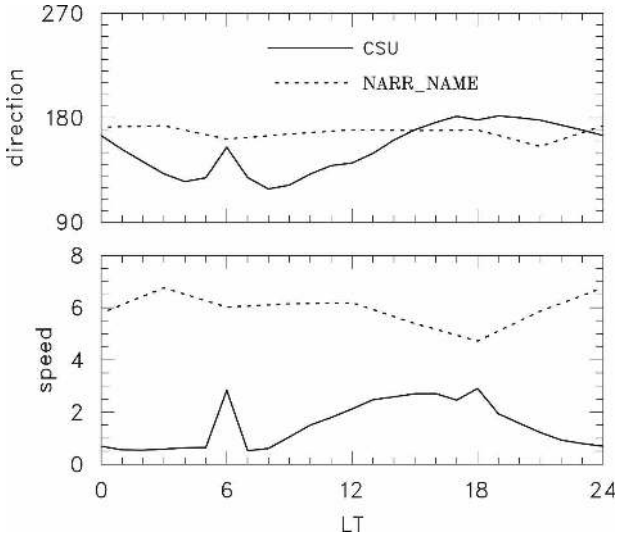

FIG. 6. EOP-mean diurnal cycle (top) wind direction and (bottom) wind speed over the northern GoC at 31°N, 114°W from the CSU (solid) and NAME_NAME (dashed) analyses. Note that at 0600 and 1800 LT QuikSCAT winds were used in the CSU analysis.

~500 m above the surface around 0600 LT (Fig. 13, Johnson et al. 2007). As noted by Douglas (1995), the GoC low-level jet usually maximizes near dawn when the relatively stable near-surface layer minimizes the jet's horizontal momentum transfer down to the surface. Over southern Arizona and New Mexico, diurnal wind variations are consistent with inertial effects superimposed on localized flows due to topographic features.

For comparison to Fig. 7, the diurnal variations of the surface wind from the NARR_NAME at several selected locations over the T1A domain are shown in Fig. 8. By design of the objective analysis scheme, the CSU winds closely resemble those observed, and thus are not presented here. As noted earlier in the wind persistence analysis (Fig. 5), the diurnal variations in NARR_NAME winds are much smaller than observed, resulting in their high persistence. At many coastal locations along the GoC, a strong southerly wind component is present, with little evidence of a land–sea breeze circulation couplet. In particular, no afternoon sea breeze is observed over the northern and central portions of Baja's east coast, which allows too much cool, dry air to be advected eastward across Baja from the eastern Pacific. Negative biases in the NARR_NAME temperatures and humidities at sites along eastern Baja range from 1° to 4°C and 3 to 5 g kg^{-1} (Fig. 4). In addition, the early morning land breeze observed along the west coast of the Mexican mainland is not present in the NARR_NAME. High persistence is also observed across southern Arizona and New Mexico, where NARR_NAME winds exhibit much less diurnal variability than observed.

TABLE 1. RMS errors between observed surface fields and analyses computed using 3-h data from the 157 quality controlled surface sites described in the text.

Variable	CSU	NARR_NAME
T_s (°C)	0.86	2.76
r_s (g kg^{-1})	0.80	2.67
u_s (m s^{-1})	1.19	1.23
v_s (m s^{-1})	1.23	2.47

TABLE 2. Biases (analyses − observed) computed using 3-h data from the 157 quality controlled surface sites described in the text.

Variable	CSU	NARR_NAME
T_s (°C)	−0.18	−0.86
r_s (g kg^{-1})	0.08	−1.37
u_s (m s^{-1})	0.13	0.33
v_s (m s^{-1})	−0.10	0.56

The observed diurnal cycles of surface temperature and dewpoint at several sites over the NAM domain are shown in Fig. 9. Over data-dense regions only a representative sampling of sites is shown. The plots with yellow background are from sites reporting routine aviation observations, which would generally be available for use in real-time analysis systems. As noted earlier, and seen here and in Fig. 7, several of these SMN sites do not report nighttime observations. The large diurnal amplitude in temperature, observed at inland sites, gradually diminishes nearer to the coastlines where the moderating effects of the seas are felt. In comparison, the diurnal amplitude of dewpoint is much smaller, with a weak afternoon minimum when surface heating and boundary layer mixing are strongest. An exception to this occurs at sites along the northern half of Baja's east coast. In this region, prominent afternoon dewpoint maxima result from an afternoon sea breeze (Fig. 7), which advects moist air off the gulf; while at night, a westerly land breeze advects drier air off the east Pacific, resulting in the observed dewpoint drop. Since the NARR_NAME does a poor job at reproducing the land–sea breeze circulation in this region, the diurnal cycle of the NARR_NAME dewpoints in this region is relatively flat (not shown).

Yet another feature of note in Fig. 9 is the small nighttime dewpoint depressions at several high elevation sites and along Baja's west coast. NARR_NAME fields show these near-saturated surface conditions at night over western Baja, but this is not the case in the NARR_NAME over the higher elevations of the SMO.

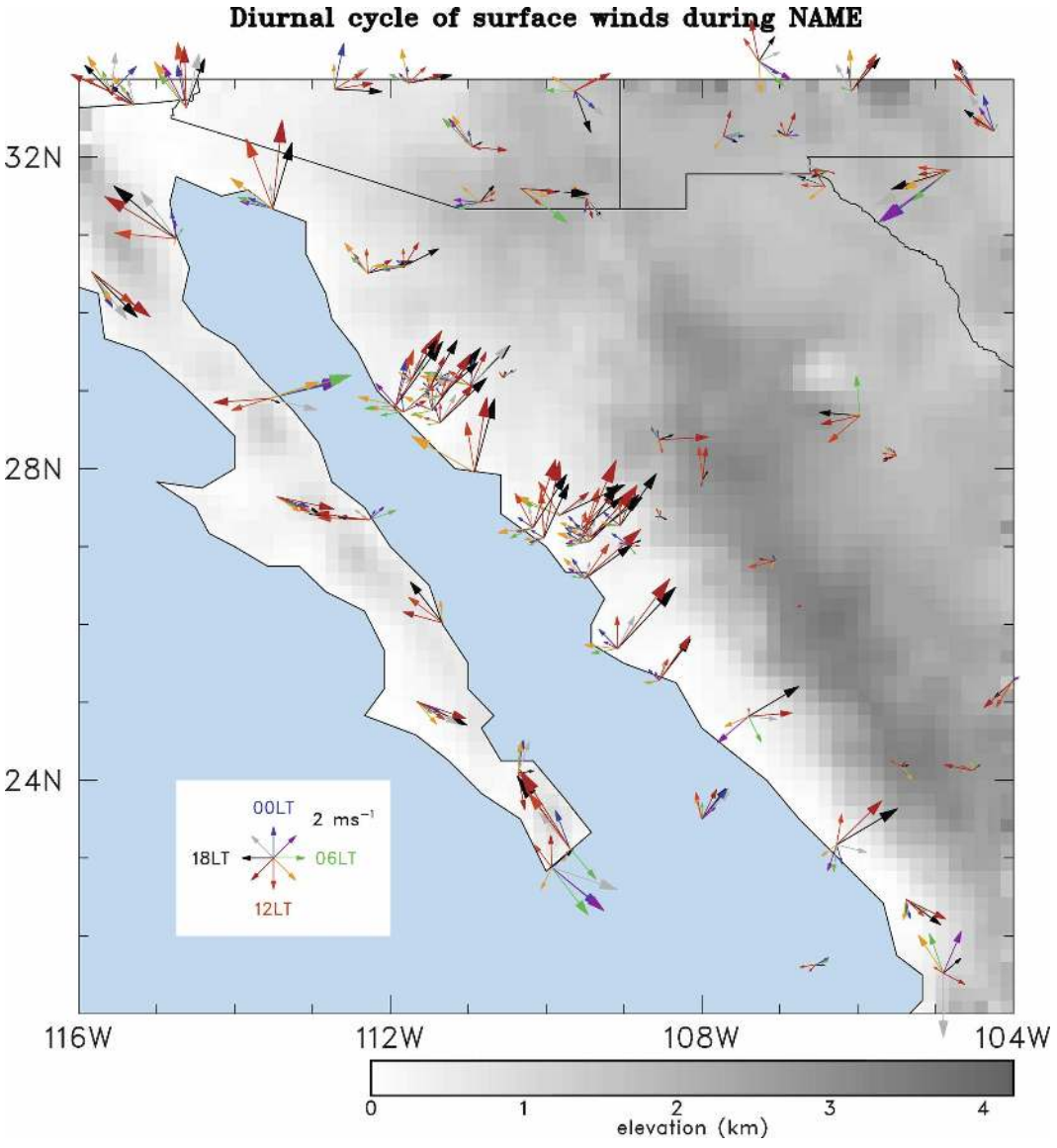

FIG. 7. EOP-mean diagrams depicting 3-h-averaged wind vectors for several surface sites within the NAME domain. Color of arrow, as shown in the notation key, indicates local time of the 3-h average.

For example, Fig. 10 (top panel) compares the observed EOP-mean diurnal cycle of dewpoint depression averaged for seven sites between 25° and 30°N located near the crest of the SMO to that computed from the NARR_NAME fields at the same locations. The observed diurnal cycle shows small depressions (1°–2°C) in the overnight hours while the dry bias in NARR_NAME results in much larger depressions (~4°C) during the night.

To illustrate how the NARR_NAME dry bias could impact convection, Fig. 11 shows the diurnal cycle of cloud-base height computed along the cross-gulf (CG) transect shown in Fig. 1 for the CSU and NARR_NAME analyses.[3] The numbers in parentheses indicate the mean cloud base height along the CG transect at different times of day. Cloud bases computed using the NARR_NAME are higher (260–459 m) at all times. Cloud bases are particularly low in the CSU analysis at night on western slopes of the SMO at higher elevations, which is consistent with the observations of frequent overnight low cloudiness (i.e., fog and stratus) in

[3] Here cloud-base height (CBH) in km is computed as CBH = $0.125(T_s - T_d)$ from Stull (1995, p. 88).

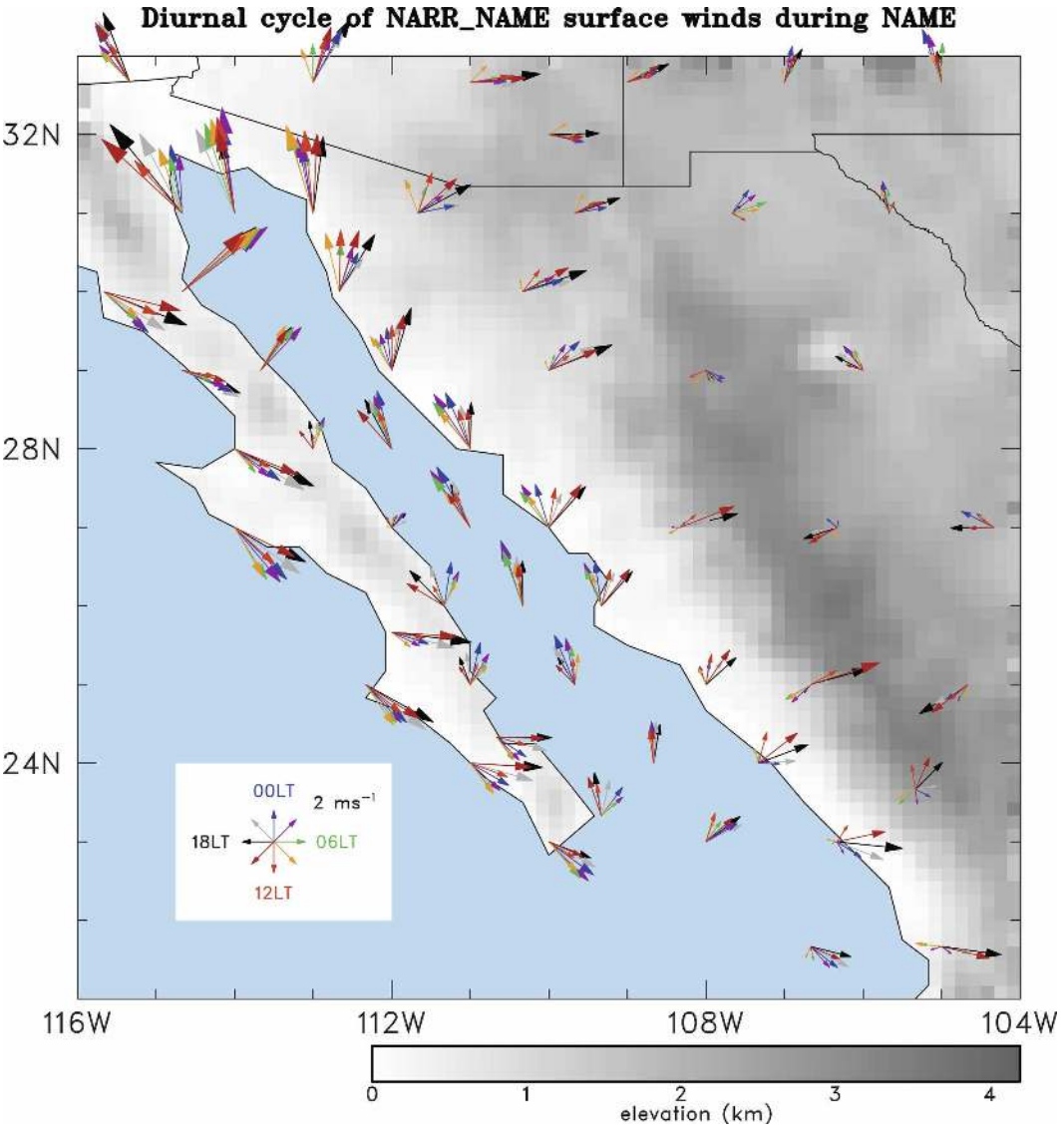

FIG. 8. EOP-mean diagrams based on 3-h NARR_NAME analyses depicting wind vectors at several locations within the NAME domain. Color of arrow, as shown in the notation key, indicates its local time.

the high terrain (Alcantara et al. 2002; Xie et al. 2005; Nesbitt and Gochis 2008).

To further investigate the development of the diurnal cycle in the monsoon core region, Figs. 12 and 13 show diurnal Hovmöller plots of various fields along the CG transect shown in Fig. 1, using the CSU and NARR_NAME gridded analyses, respectively. The location of this transect was chosen to be representative of the monsoon core while making optimal use of the data sampling. Comparison of the temperature plots (top panels) shows the cool bias in the NARR_NAME, which is most obvious at higher elevations during the night. This feature is likely a consequence of the NARR_NAME dry bias that results in less nighttime cloudiness over the higher terrain and thus enhanced radiative cooling in the overnight hours. The NARR_NAME cool bias is also observed over the coastal plain during the day where the 30°C isotherm in the CSU analysis covers a larger region extending up the west slope of the SMO.

The second set of panels shows the response to these temperature fields given in terms of the cross-gulf wind (i.e., the component of the flow in the plane of the cross section). The CSU analysis (Fig. 12) shows a weak land breeze (negative values or offshore flow) centered near the coast from 0000 to 0900 LT transitioning to a sea breeze (positive values or onshore flow) that peaks in the late afternoon. These observations of the sea and

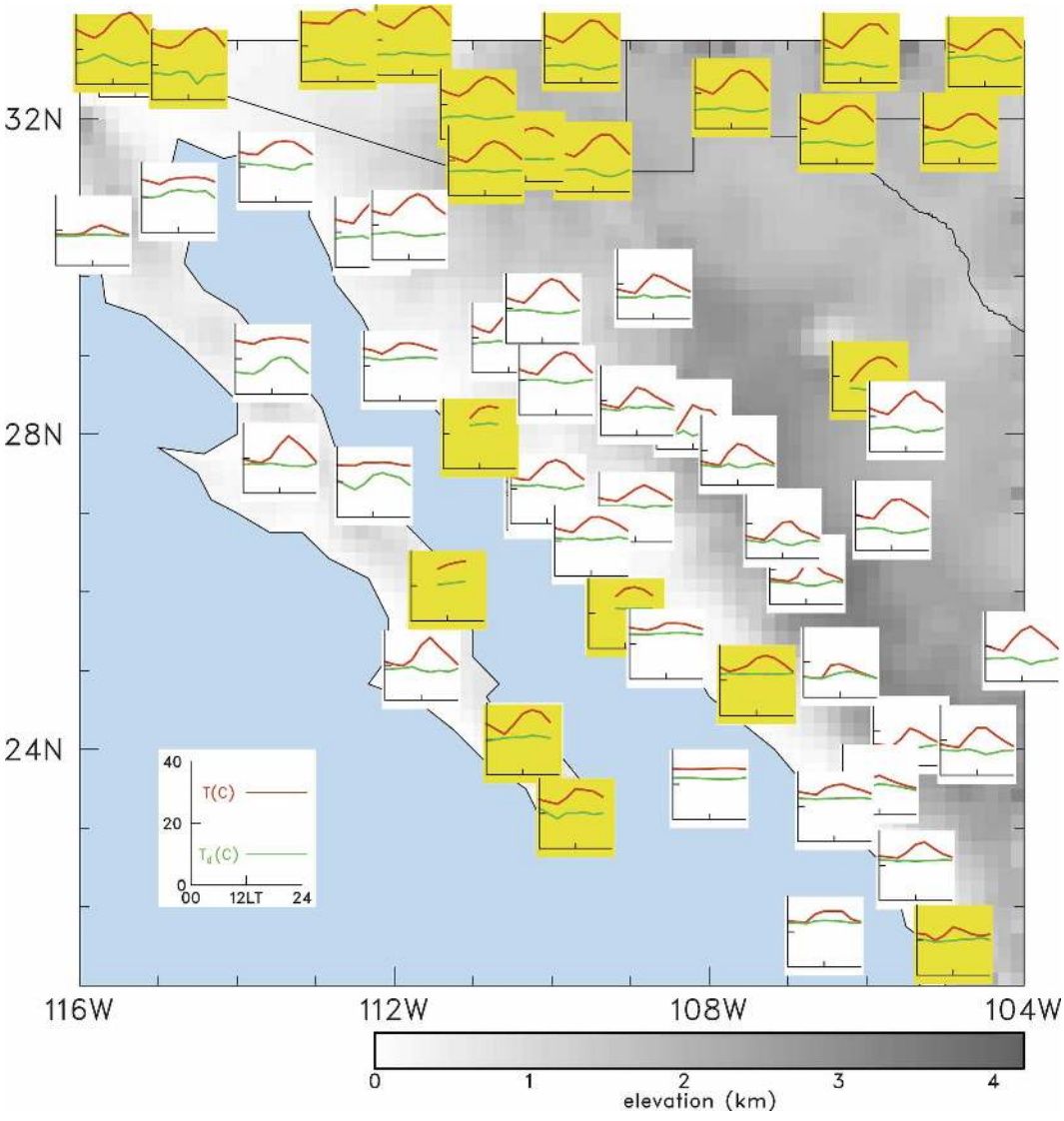

FIG. 9. EOP-mean diurnal cycle of temperature (red curve) and dewpoint temperature (green curve) for several surface sites within the NAME domain. Yellow shading indicates that sites are from routine aviation observations that would generally be available for use in real-time analyses.

land breezes being centered near the coast are consistent with earlier modeling and observational studies (e.g., Wexler 1946; Mahrer and Pielke 1977). During the daytime hours, the CSU analysis shows weak (~1 m s^{-1}) upslope flow extending up the west slopes of the SMO, while at night downslope winds are less than 0.5 m s^{-1}. These observations corroborate the notion of Nesbitt and Gochis (2008) that the presence of high-terrain nocturnal clouds limits radiational cooling and thus nocturnal downslope flows.

In contrast, NARR_NAME winds (bottom panel of Fig. 10 and Fig. 13) are generally stronger than those in the CSU analysis. Most notably, the NARR_NAME shows much stronger nocturnal downslope (westward) flow over the higher western slopes of the SMO. However, this westward flow does not extend to the coast, so no land breeze is observed. During the daylight hours, two onshore wind maxima are present: one about ~100 km inland at 1500 LT and a second slightly weaker peak ~40 km inland at 1800 LT, presumably a reflection of the sea breeze. The stronger nighttime downslope flow in the NARR_NAME likely results from the NARR_NAME's dry bias that, as mentioned earlier, would result in less nighttime cloudiness and stronger radiative cooling. This lack of nighttime cloudiness could also result in a more rapid warmup of the higher peaks and

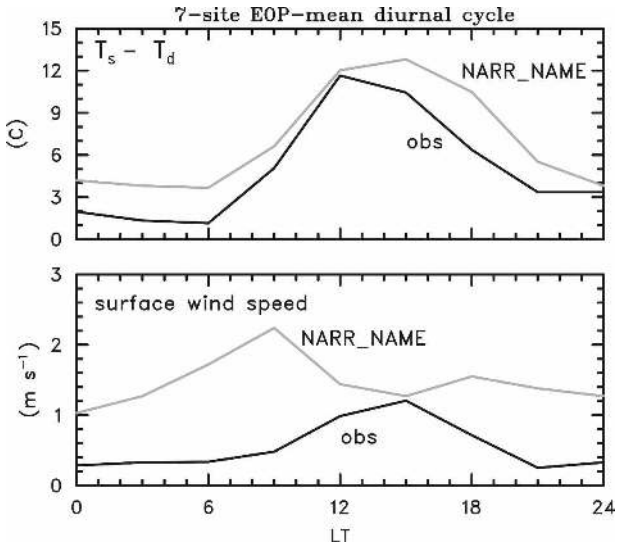

FIG. 10. Seven-site, EOP-mean diurnal cycle of (top) dewpoint depression and (bottom) wind speed. Black curves denote actual observations; gray curves represent NARR_NAME analysis interpolated to station locations. Stations used here represent high-elevations sites (mean elevation 2180 m) between 25° and 30°N.

the stronger daytime upslope flow seen in the NARR_NAME. An alternative explanation for these stronger daytime upslope flows may be that, to compensate for the dry bias in the NARR_NAME, the model must

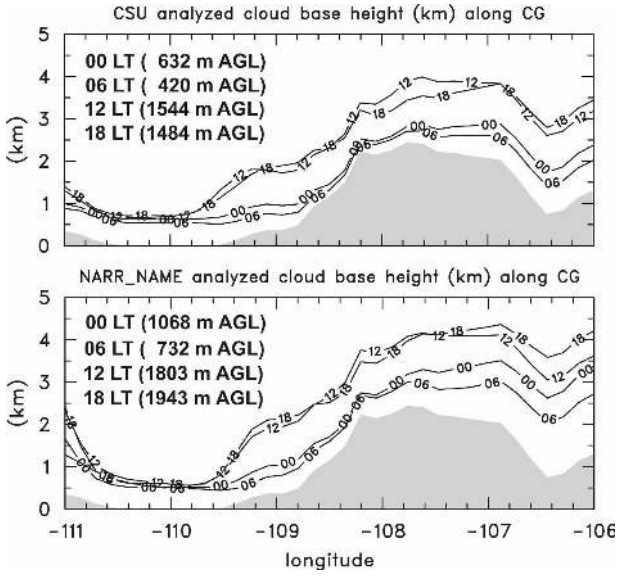

FIG. 11. EOP-mean cloud base height (km) along the CG transect computed (top) using CSU temperature and dewpoint fields and (bottom) using NARR_NAME fields. Numbers along curves indicate the local time. Numbers in parentheses indicate the mean cloud base height AGL at different times of day for areas over land (i.e., east of 109.5°W). Elevation along this transect is shaded.

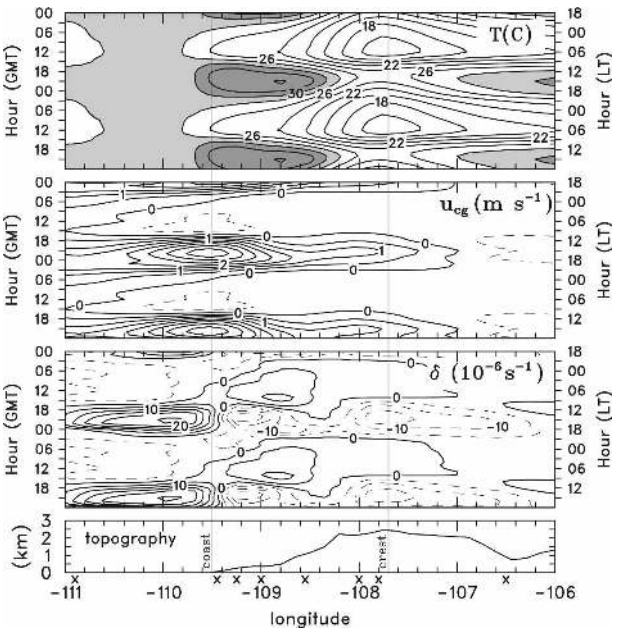

FIG. 12. Time of day vs longitude plots along CG transect shown in Fig. 1 computed from CSU surface analyses: (top) temperature, (second panel) the wind component in the plane of transect (u_{cg}), and (third panel) divergence. Contour interval is 2°C for temperature, 0.5 m s^{-1} for u_{cg}, and 5×10^{-6} for divergence. Data used in constructing plots were from the NAME EOP (1 Jul–15 Aug 2004). (bottom) The height of the topography along the transect with x denoting the location of observing stations. Thin vertical lines indicate the location of the west Mexican coast and crest of the SMO in the CG transect.

generate stronger upward vertical motions to initiate and sustain convection in the assimilation process in order to match the observed precipitation.

The third panel in Figs. 12 and 13 shows the diurnal cycle of the surface divergence field. The main features to note in the CSU analysis are the strong daytime divergence over the GoC, related to the diverging sea-breeze circulations, and the two daytime convergence regions over land. The convergence region located just west of the SMO crest begins to develop around 0900 LT. This region of surface convergence is likely related to the formation of shallow convection over the higher peaks as observed by radar (Lang et al. 2007) and detected in gauge data (Gochis et al. 2004; Nesbitt and Gochis 2008). The second region of convergence, which peaks in the early afternoon about ~40 km inland, is related to the sea-breeze front and results in a coast-parallel band of convection as observed by radar (Nesbitt and Gochis 2008). The NARR_NAME also shows a strong daytime divergence over the GoC and convergence over the upper slopes of the SMO, but many of its other features bear little resemblance to those in the CSU analysis.

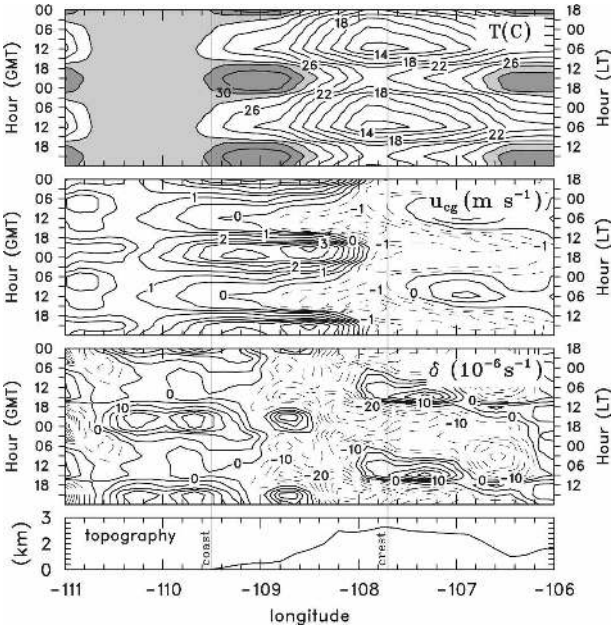

FIG. 13. As in Fig. 12 but computed from NARR_NAME surface analyses.

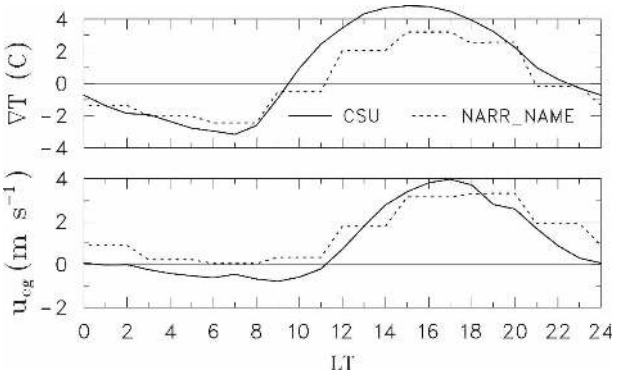

FIG. 14. (top) Temperature gradient and (bottom) cross-gulf winds at coast along the CG transect shown in Fig. 1. Temperature gradient computed as T_s difference between land (first inland point) and gulf (second offshore point) such that a positive difference means the land is warmer than the gulf. Positive (negative) u_{cg} indicates onshore (offshore) flow where u_{cg} is measured at the first inland point.

To examine the details of the land–sea breeze circulation, Fig. 14 shows the diurnal cycle of the cross-gulf temperature gradient and winds at the west Mexican coast along the CG transect. This central gulf transect is well representative of other coastal locations that were examined but not shown here. The stepwise nature of the NARR_NAME curves is related to its 3-h resolution compared to the 1-h resolution of the CSU analysis. The characteristics of the NARR_NAME temperature gradient generally resemble those in the CSU analysis with peak negative values (gulf warmer than land) around 0700 LT, a changeover to positive values a few hours later, and peak positive values around 1500 LT. While the amplitude of the negative gradient is about the same in both analyses, the daytime positive gradient is about 40% less in the NARR_NAME, reflecting its daytime cool bias over the coastal land region. In the CSU analysis the peak land breeze ($u_{cg} < 0$) and peak sea breeze ($u_{cg} > 0$) occur at 0900 and 1700 LT, respectively, lagging the peak temperature gradients by about 2 h. While the NARR_NAME sea breeze is of comparable strength to that in the CSU analysis, the NARR_NAME does not exhibit a land breeze even though its temperature gradient appears strong enough to support one.

Since one of the primary motivations for creating a high quality surface wind analysis was to capture slope flows as accurately as possible, Fig. 15 shows the diurnal evolution of vertical motion at the surface, computed using the CSU wind analysis and Eq. (1). During the early morning hours the development of a land breeze over western Mexico results in a weak downslope flow ($\omega_s > 0$) over this region. This downslope flow peaks ~3–4 hPa h^{-1} at 0900 LT when the land breeze is at its strongest (Fig. 14). By 1200 LT the developing sea breeze results in a weak rising motion just inland. This upslope flow increases and spreads eastward (Fig. 12) during the course of the afternoon resulting in a maximum upward motion ~12 hPa h^{-1} around 18 LT. After this time the upslope flow quickly weakens and is replaced with weak flows (±1 hPa h^{-1}) by midnight. As implied earlier, but shown here explicitly, nighttime downslope flow over the higher elevations of the SMO are quite weak (generally less than 1 hPa h^{-1}).

To obtain a larger-scale perspective on the diurnal cycle, Fig. 16 compares the NARR_NAME and CSU analyses of several fields averaged over a region covering much of northwestern Mexico (denoted as NWM in Fig. 1). This region encompasses the area east of the GoC from the west mainland coast to the crest of the SMO. While the cool and dry bias in the NARR_NAME is clearly seen (Fig. 16, top two panels), the diurnal phase and amplitude of these two analyses are in good agreement. This is also true of the diurnal cycle of the cross-gulf wind component, u_{cg} (Fig. 16, middle panel), which shows a significant positive bias in the NARR_NAME.[4] Despite the large differences in diver-

[4] Here the cross-gulf wind component was computed assuming the angle of the GoC from north was 35°, such that $u_{cg} = u \times \cos(35) + v \times \sin(35)$. This wind component represents the flow perpendicular to the coast and, thus, is used to describe the strength of the land–sea breezes.

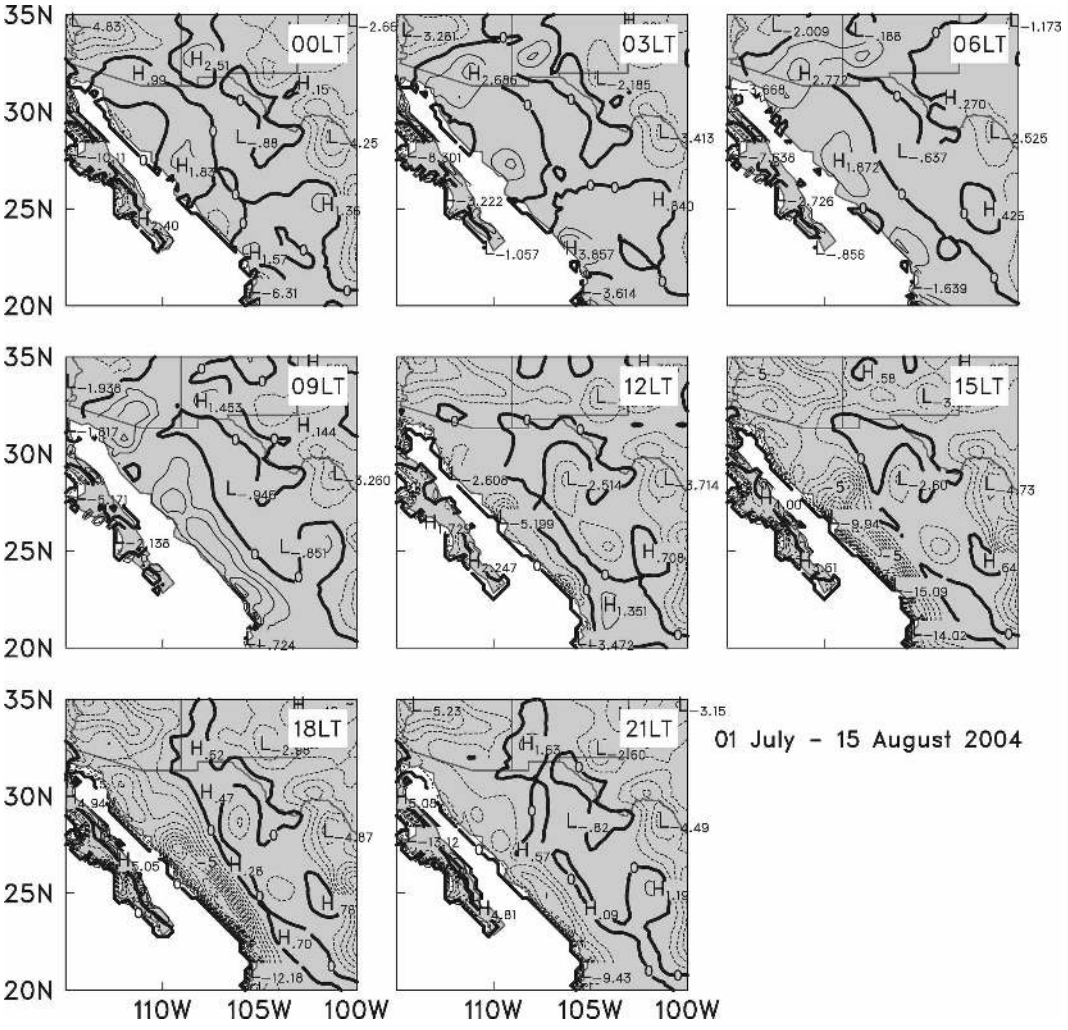

FIG. 15. Diurnal cycle of vertical motion at the surface for NAME EOP computed from the CSU analysis. Contour interval is 1 hPa h^{-1} where positive (negative) contours denote sinking (rising) motion.

gence between the analyses along the CG transect shown in Figs. 12 and 13, the diurnal cycle of the divergence and vertical motion averaged over this large region shows some level of agreement (Fig. 16, bottom two panels). Both analyses exhibit weak nighttime divergence and vertical motions over the NWM region transitioning to strong surface convergence and rising motion as the sea breeze develops. However, a notable difference in these analyses is that this transition begins at about 0600 LT in the NARR_NAME compared to 0900 LT in the CSU analysis. The added burst of divergence and subsidence in the CSU analysis between 0600 and 0900 UTC coincides with the peak in the land breeze over western Mexico (Figs. 7 and 12), which is largely missing in the NARR_NAME. Despite the strong constraints placed on the NARR_NAME by assimilating observed 3-h precipitation (Mesinger et al. 2006), these results indicate the NARR_NAME's tendency to initiate the daily convective cycle too early, similar to what is observed in the Eta Model and Global Forecast System (GFS) operational models over this region, which reach their convective maxima ~3 h earlier than observed (Janowiak et al. 2007). Finally, we suggest that the biases in u_{cg} and the stronger convergence and rising motion in the NARR_NAME are likely a consequence of its analysis scheme's attempt to compensate for the lack of low-level moisture by generating a large-scale environment conducive to more vigorous convection.

5. Evolution of surface diurnal cycle

Following the onset of monsoonal rains, the vegetation characteristics over large portions of the NAME

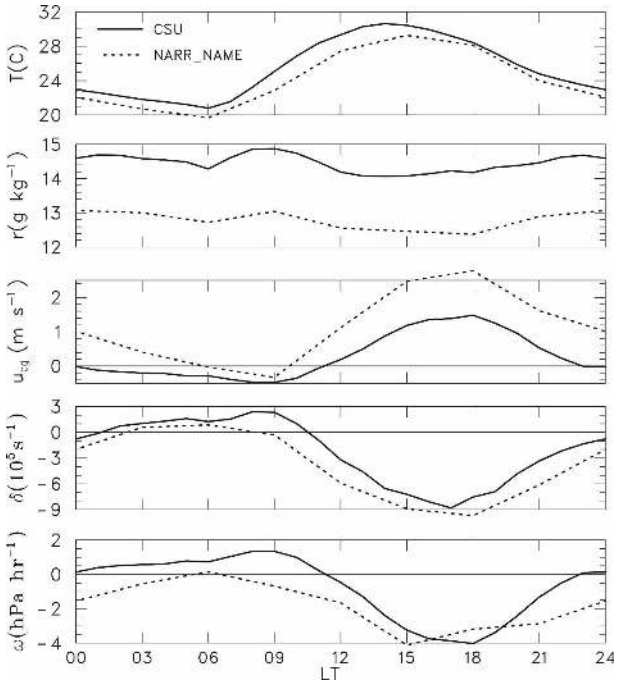

FIG. 16. Diurnal cycle of surface fields over the NWM region (polygon shown in Fig. 1) during the NAME EOP: (top) temperature, (second panel) water vapor mixing ratio, (middle panel) cross-gulf wind component, (fourth panel) divergence, and (bottom) vertical motion. CSU analysis shown in solid curves; NARR_NAME shown in dashed.

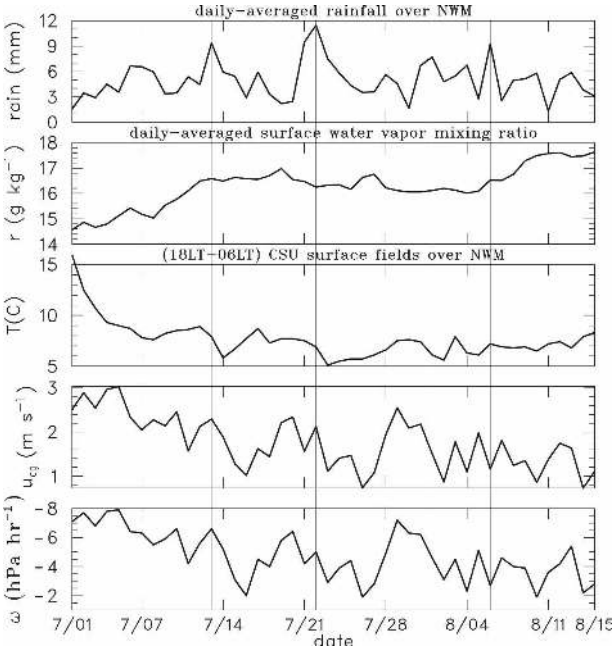

FIG. 17. Time series during the NAME EOP of various CSU-analyzed surface fields averaged over the NWM region shown in Fig. 1: (top) daily averaged TRMM 3B42 rainfall, (second panel) daily averaged water vapor mixing ratio, (middle panel) amplitude of the diurnal cycle (value at 1800 LT minus that at 0600 LT) for temperature, (fourth panel) cross-gulf wind, and (bottom) vertical motion. Vertical lines indicate days with rainfall rates >8 mm day^{-1}.

region undergo dramatic changes. For example, during the period from 10 to 20 July 2004, Watts et al. (2007) found huge increases in vegetation indices at two sites in Sonora, Mexico, indicating rapid foliation in the deciduous forest and shrublands of this region. Using data from seven pilot balloon sites over Baja and along the coast and foothills of western Mexico, Douglas et al. (2006) presented preliminary analyses on the seasonal evolution of low-level winds over this region and speculated on their link to vegetation green-up. As an extension to the Douglas study, this section examines the evolution of the diurnal cycle in various surface fields as the monsoon progresses. The results presented in this section are based on the CSU surface analysis, which has the advantage of having higher temporal resolution than the NARR_NAME (1 versus 3 h), and, as shown above, generally provides a more realistic description of the surface fields. Despite the limitations of the NARR_NAME surface analyses, the results shown in this section based on the CSU analysis generally agree with those from the NARR_NAME unless noted otherwise.

To document how surface fields are impacted by monsoonal rains, Fig. 17 shows the time series of TRMM-estimated rainfall along with several fields averaged over the NWM region (shown in Fig. 1). Rainfall over this region gradually increases early in the NAME EOP as the monsoon progresses northward. The vertical lines in Fig. 17 denote rainfall events with daily averaged rates greater than 8 mm day^{-1}. The first two of these events in mid July were associated with major gulf surges that advected cool, moist air northward into the deserts of the southwestern United States and northwestern Mexico. Water vapor mixing ratios (second panel in Fig. 17) rapidly increase during the first two weeks of the EOP to ~16.5 g kg^{-1}, level off for several days, then continue to rise during the last few weeks of the EOP. The remaining panels in Fig. 17 show how the amplitude of the diurnal cycle of surface temperature, cross-gulf winds, and vertical motion vary in response to these fluctuations in rainfall and moisture. Here the diurnal amplitude is estimated by taking the difference between values at 1800 and 0600 LT. While this simple measure does not capture the full range of the diurnal cycle (e.g., Fig. 16 shows temperatures peaking ~1400 LT), it is adequate for determining trends.

The diurnal amplitude of all these fields is largest near the beginning of the EOP, prior to onset of the

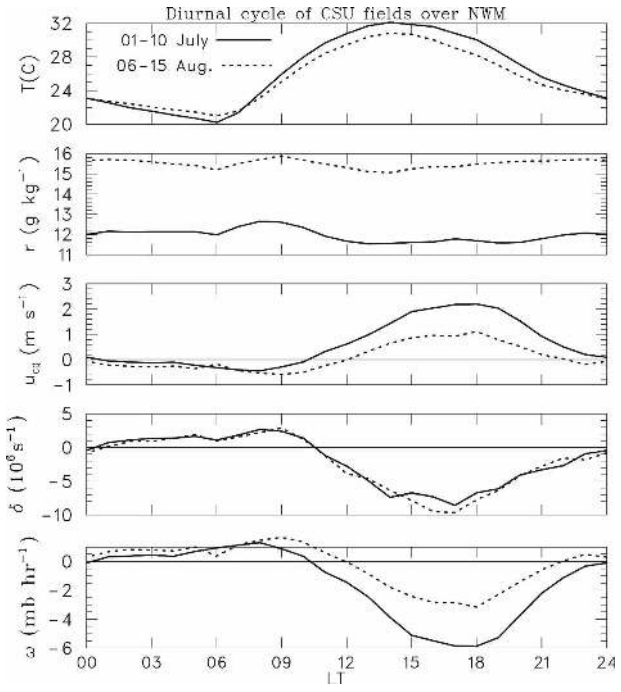

FIG. 18. Diurnal cycle of CSU-analyzed surface fields averaged over the NWM region shown in Fig. 1 for the 10-day period at beginning of NAME EOP (solid curve) and for the 10-day period at the end of NAME EOP (dashed curve).

heavy rains and moist surface conditions. This is especially evident in the temperature field in which its diurnal amplitude decreases from 16° to 8°C during the first week of the EOP. This amplitude decrease is less dramatic in the NARR_NAME going from 12° to 9°C (not shown). Following each major rain event, the diurnal amplitude of these fields decreases, although the amplitude reduction becomes more muted as the monsoon progresses. Correlations between daily averaged rainfall and the temperature diurnal amplitude are −0.31 and −0.34 at lag 0 and 1 day, respectively. The negative correlation at day 0 is likely due to enhanced cloudiness, while its persistence the following day suggests that more solar radiation is going into evapotranspiration and less into sensible heating. Correlations between the diurnal amplitude of temperature and u_{cg} are ~0.6 at lag 0, 1, and 2 days. In other words, following significant rain events the muted daytime heating over land results in a weaker land–sea breeze circulation and sloped flows. The lag day-0 correlation between the diurnal amplitudes of u_{cg} and surface vertical motion is 0.97, which indicates that surface flows perpendicular to the coast are primarily responsible for generating surface vertical motions over the NWM region.

To highlight the changes in the diurnal cycle as the monsoon progresses, Fig. 18 shows the diurnal variation of several surface fields averaged over the first and last 10 days of the NAME EOP. These two periods, which do not contain any of the major rain events during the EOP, should be long enough to minimize synoptic-scale effects. During the early monsoon period the amplitude of the temperature diurnal cycle (based on the 1400 and 0600 LT difference) was ~12°C (Fig. 18, top panel). The decrease in amplitude to ~9°C in the late period is due mainly to less daytime warming. The reduction in both the daytime warming and nighttime cooling over the NWM region as the monsoon progresses likely results from a combination of factors. As speculated by Douglas et al. (2006), these factors include increased soil moisture, larger values of evapotranspiration as the dry vegetation leafs out, and increased cloud cover. While the amplitude of the water vapor mixing ratio diurnal cycle (Fig. 18, second panel) exhibits little change over the course of the monsoon, the mean values show nearly 4 g kg^{-1} of moistening.

The impact of these temperature and moisture changes on the circulation are shown in the bottom three panels in Fig. 18. The diurnal amplitude of the cross-gulf winds (middle panel) decreases by more than 50% from the early to the late period, due to a substantial weakening of the afternoon onshore flow ($u_{cg} > 0$) in the late period. In fact, during the later period the early morning offshore flow ($u_{cg} < 0$) is slightly stronger and persists later into the morning, possibly due to a warmer GoC. SSTs in the central GoC rose about 1.5C during the NAME EOP (see Fig. 5 in Wang and Xie 2007). Somewhat surprisingly, considering the reduction in the u_{cg} winds, afternoon convergence shows a slight increase during the later period (Fig. 18, fourth panel). Upon closer inspection, we found that this divergence increase occurs primarily in a 50-km-wide strip along the coast (not shown). Thus, as discussed in Douglas et al. (2006), the weaker sea breeze, warmer GoC, and increased convergence near the coast in the later period favor the preferred region for convective development toward the coast. Finally, a large decrease in the afternoon upslope flow during the later period is noted (Fig. 18, bottom panel), consistent with the weakened onshore flow.

To examine changes in the surface flow over a larger portion of the NAME domain, Fig. 19 shows surface maps of the CSU wind vectors at 0600 and 1800 LT and their difference for two 10-day periods early and late in the NAME EOP. As a reminder, most of the wind data over the GoC and Pacific going into this analysis come from the QuikSCAT winds that are available during these hours. Several features in Fig. 19 are worth noting. At all times a strong northwesterly flow is observed running parallel to the west coast of Baja. At 1800 LT

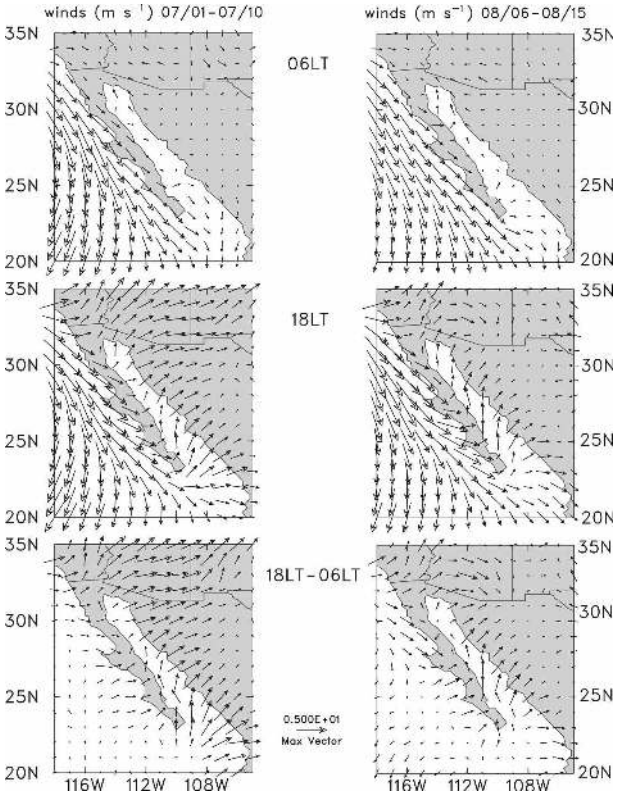

FIG. 19. CSU wind analyses for two 10-day periods at the (left) start and (right) end of NAME EOP. Wind analyses for (top) 0600 LT, (middle) 1800 LT, and (bottom) the difference (1800 − 0600 LT).

these northwesterlies flow around the tip of Baja and appear to fan out, with a portion of the flow continuing southeasterly, some flowing westerly into Mexico, and the remainder turning northwesterly up the GoC. The main difference between the two periods, seen most readily at 1800 LT, is the stronger flow directed toward the continent in the early period. In fact, at 1800 LT stronger winds are observed nearly everywhere in the early period, especially over the southwest United States and the west slopes of the SMO. Looking at the diurnal difference maps, the early period shows a strong land–sea breeze circulation along the west coast of the Mexican mainland extending eastward well up the slopes of the SMO. Also during the early period, the influence of the land–sea breeze circulation can be seen well offshore, in places extending out 300–400 km from the coast. During the later period, the land–sea breeze circulation is still present along the coast, albeit weaker and more limited in extent in both directions. In contrast, the diurnal difference maps created using NARR_NAME winds (not shown) exhibit no appreciable changes in the horizontal extent of the land–sea breeze circulation as the monsoon progresses.

A similar study on the diurnal cycle of surface winds in the NAME region was conducted by McNoldy et al. (2006), but in their analysis only QuikSCAT winds were used with slightly different averaging periods. Defining the early monsoon period to be 1–21 June 2004, their diurnal difference maps showed the land–sea breeze circulation extending up to 500 km offshore. Vegetation index maps presented in Fig. 2 of Watts et al. (2007) show that land surface green-up had begun by early July over the southern NAME domain, which may explain the more limited offshore extent of the land–sea breeze circulation in our early July analysis. A notable difference between the analyses in Fig. 19 and McNoldy et al., is that the later study, as well as the NARR_NAME (see Fig. 6), show the presence of stronger southerly winds over the northern GoC at 0600 LT compared to 1800 LT. These weaker southerlies at 0600 LT in the CSU analysis result from analysis times when no QuikSCAT winds were available over the northern GoC (~30% of the time). At these times, the CSU winds over the gulf represent an interpolation from winds at coastal sites that do not exhibit an early morning southerly maximum (see Fig. 7).

6. Surface fluxes

With essentially no surface energy flux measurements over Mexico prior to NAME (Zhu et al. 2007), it was recognized that an important component to understanding and better prediction of the NAM was documenting the fluxes of energy that occur near the earth's surface. During NAME, surface fluxes were measured at a variety of locations including seven sites over Sonora, Mexico, and southern Arizona (Watts et al. 2007); on the R/V *Altair* at the mouth of the GoC (Zuidema et al. 2007); and at Obispo, Sinaloa (L. Hartten 2007, personal communication). In this section, sensible heat (SH) and latent heat (LH) fluxes from these latter two sites are compared to fluxes from the NARR_NAME. At the time of this study, flux data from the Watts et al. (2007) sites were not available for this comparison.

The R/V *Altair* was positioned at the mouth of the Gulf of California for much of the NAME EOP from 7 July to 11 August with a short port call from 22 to 27 July. The observations taken at the *Altair*, which are summarized in Zuidema et al. (2007), included the measurement of surface fluxes obtained through the bulk aerodynamic method (Fairall et al. 1996). For comparison to the 3-h NARR_NAME fields, the 5-min *Altair* fluxes were averaged in 3-h periods. A time series of daily averaged latent and sensible heat fluxes is presented in the Zuidema et al. paper (their Fig. 8) and is

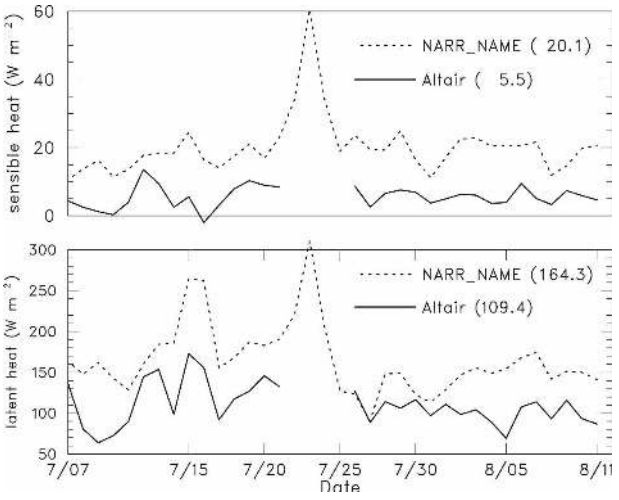

FIG. 20. Time series of daily averaged (top) sensible and (bottom) latent heat fluxes from observations taken at the R/V *Altair* (solid line) and NARR_NAME data interpolated to the *Altair*'s location (dashed line). Numbers in parentheses represent the mean flux values for the 32 days when the *Altair* was on site at the mouth of the gulf.

reproduced in Fig. 20 along with a comparison to the NARR_NAME fluxes interpolated to the *Altair*'s position. Enhanced fluxes are observed in both time series during two strong July gulf surges, around 13 and 23 July. Zuidema et al. noted that the low-level winds reached 12 m s^{-1} during this first surge. While the day-to-day variability in these time series tracks reasonably well, there is a large positive bias in the NARR_NAME fluxes (~14 W m^{-2} for sensible heat and ~55 W m^{-2} for latent heat). The ~1°C cool bias in the NARR_NAME temperature field (see Fig. 2, top-right inset) may partially account for its larger sensible heat fluxes. On the other hand, the fields that could account for the large latent heat flux differences (r_s, SSTs, and wind speeds) are quite similar in both analyses (see insets in Fig. 2 and Table 3 for their mean values), which suggests that the flux formulation in the NARR is different from that used by Fairall et al (1996).

Yet another explanation for the excessive NARR_NAME fluxes comes from an examination of the surface energy budget, which reveals that the downward shortwave (DSW) radiation component in the NARR_NAME was 38 W m^{-2} larger than that observed at the *Altair*. This higher DSW may in turn be related to difficulties the model has in dealing with clouds and aerosols. Thus, the enhanced latent and sensible heat fluxes seen in the NARR_NAME may represent the mechanism by which the land surface model (LSM) attempts to balance this radiation surplus.

The diurnal cycles of sensible and latent heat fluxes

TABLE 3. Mean values of surface fields at the R/V *Altair*. NARR_NAME values were interpolated to location of the *Altair*.

Variable	Observed	NARR_NAME
SST (°C)	30.3	30.2
T_s (°C)	28.9	28.0
r_s (g kg^{-1})	18.2	18.1
$\|u\|_s$ (m s^{-1})	3.5	3.4
SH (W m^{-2})	6	20
LH (W m^{-2})	109	164

observed at the *Altair* and computed from the NARR_NAME (Fig. 21) clearly show the large positive biases in the NARR_NAME fluxes. The sensible heat flux exhibits a very slight diurnal variation (~1 W m^{-2} in the *Altair*, ~3 W m^{-2} in the NARR_NAME). In comparison the diurnal variation in latent heat flux is more substantial (~17 W m^{-2} in the *Altair*, ~37 W m^{-2} in the NARR_NAME) with peak values occurring in the late afternoon and evening. At this time of day the sea breeze is well established over western Mexico and Baja (Figs. 7 and 19), causing strong low-level divergence over the GoC (Fig. 12). This diverging wind pattern results in low-level subsidence over the gulf (Johnson et al. 2007), which transports drier and warmer air toward the surface (see insets in Fig. 2), leading to the enhanced surface fluxes. The peak fluxes in the NARR_NAME occur about 3 h later than those observed at the *Altair*. This is consistent with the divergence pattern observed over the GoC in Figs. 12 and 13, where the CSU analysis shows a sharp divergence peak around 1500 LT but the NARR_NAME extends this

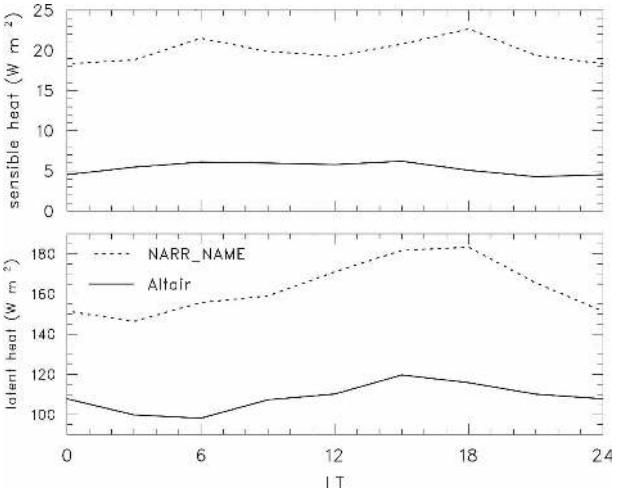

FIG. 21. Diurnal cycle of (top) sensible and (bottom) latent heat fluxes from observations taken at the R/V *Altair* (solid line) and NARR_NAME data interpolated to the *Altair*'s location (dashed line).

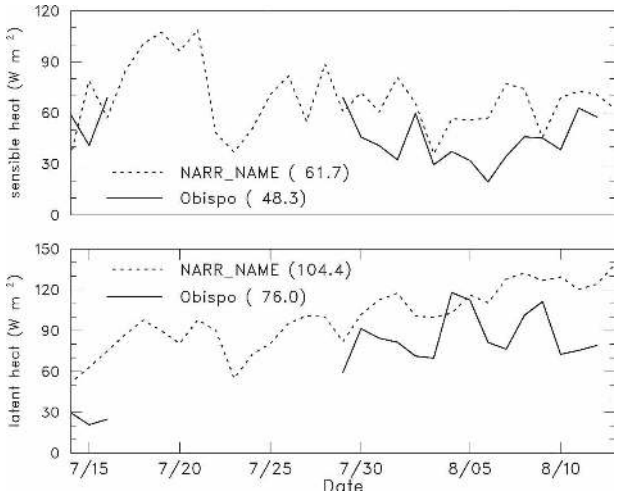

FIG. 22. As in Fig. 20 but from observations taken at Obispo, Sinaloa (solid line), and NARR_NAME data interpolated to Obispo's location (dashed line). Numbers in parentheses represent the mean flux values for the 17 days when the data at Obispo was available during the NAME EOP.

period of strong divergence to 1800 LT. As a result, the r_s minimum at the *Altair* location occurs about 3 h later in the NARR_NAME (Fig. 2).

Located about 20 km from the GoC and near its mouth, the Obispo site (location shown in Fig. 1) took surface observations from 13 July to 20 September. The data presented here is part of a multiyear study at this site. To facilitate its comparison to the 3-h NARR_NAME data, the 2-min surface data and 30-min flux data from this site were averaged into 3-h bins. The time series of surface fluxes at Obispo and for the NARR_NAME interpolated to this location are shown in Fig. 22. Unfortunately, instrumentation failure during the NAME EOP (see data gaps in Fig. 22) resulted in only 17 days of reliable flux data at the Obispo site. In comparison to the *Altair*, on average the Obispo sensible fluxes are nearly a factor of 10 larger (5.5 versus 48) due to large daytime heating of the land. The Obispo latent heat fluxes, which are small initially, are of comparable magnitude to the *Altair*'s by early August. Despite the sparse data sampling early in this period, the large increase in the latent heat flux at the Obispo site as the monsoon progresses is intriguing. Similar increases in evapotranspiration were documented by Watts et al. (2007) at several of the sites in their study and, hopefully, additional years of data from Obispo will be able to better document these dramatic flux changes during the course of the monsoon.

While the overall trends in Obispo's fluxes are captured by the NARR_NAME, a positive bias in the NARR_NAME fluxes is present (~14 W m^{-2} for sensible heat and ~28 W m^{-2} for latent heat). As seen in Table 4, which lists the mean values of the surface fields at Obispo and the NARR_NAME for the period of interest, a significant cool and dry bias is observed in the NARR_NAME fields. These biases are likely contributing to the larger NARR_NAME fluxes at the Obispo site. Furthermore, the fact that these cool and dry NARR_NAME biases extend over a significant portion of the NAME land domain (Figs. 3 and 4) suggests that the NARR_NAME may be overestimating these fluxes over a much larger region as well. Similar to the situation at the *Altair*, the DSW radiation at the surface in the NARR_NAME was ~40 W m^{-2} larger than that observed at Obispo, which likely contributes to the excessive NARR_NAME surface heat fluxes at this site. The large decrease in NARR_NAME fluxes around 23 July (Fig. 22) is related to a strong gulf surge at this time, which was accompanied by cloudy, cool, and moist conditions with little wind speed increase (not shown). These conditions effectively dampened the surface diurnal heating cycle at Obispo for a few days, resulting in the diminished fluxes.

TABLE 4. Mean values of surface fields at Obispo, Sinaloa. NARR_NAME values were interpolated to the Obispo location.

Variable	Observed	NARR_NAME
T_s (°C)	29.0	26.8
r_s (g kg^{-1})	18.3	16.4
$\|u\|_s$ (m s^{-1})	2.3	2.3
SH (W m^{-2})	48	62
LH (W m^{-2})	76	104

The diurnal cycles of sensible and latent fluxes observed at Obispo and computed from the NARR_NAME are shown in Fig. 23. In contrast to the relatively small diurnal amplitude at the *Altair* (Fig. 21), the Obispo site exhibits large diurnal variations in these fluxes (~130 W m^{-2} in the sensible flux and ~190 W m^{-2} in the latent flux) related to the strong daytime heating. The NARR_NAME, which has a large daytime positive bias, exhibits a diurnal amplitude ~250 W m^{-2} in both fluxes and a premature diurnal ramp up. Such behavior could be related to an improper specification of soil type in the NARR's LSM, which would affect how quickly the soil heats up and gives up its moisture. The soil type along the coastal plain in which the Obispo site was located is predominately clay, which is slow to heat up and release moisture (R. Zamora 2007, personal communication.) Finally, we note that this premature release of energy into the boundary layer is also likely related to the NARR's tendency to initiate convection too early in the day.

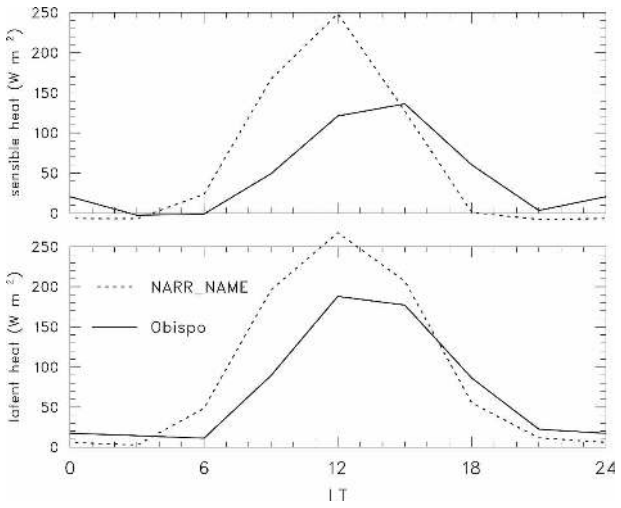

FIG. 23. As in Fig. 21 but from observations taken at Obispo, Sinaloa (solid line), and NARR_NAME data interpolated to Obispo's location (dashed line).

7. Summary and concluding remarks

Surface data collected during the 2004 North American Monsoon Experiment (NAME) have provided an opportunity to document the structure and properties of the surface flow within the North American monsoon (NAM) with detail not previously possible. Observations from 157 surface sites over the NAM domain along with twice-daily QuikSCAT oceanic winds have been quality controlled and processed into gridded datasets (referred to here at the CSU analyses) at 1-h, 0.25° resolution for the period from 1 July to 15 August. Whereas these gridded datasets cover the NAME Tier 2 domain (15°–40°N, 90°–120°W), the analyses presented in this paper focus on results for the more regional scale T1A domain, which represents the core monsoon region. One of the motivations for creating this dataset was to provide accurate analyses of surface winds for computation of vertical motion over sloped topography. These vertical motion analyses along with the other surface fields provide the lower-boundary data for an upper-air gridded dataset that will used in future studies. The CSU surface gridded dataset is available online (http://tornado.atmos.colostate.edu/name).

The main goals of this study are to document the mean, temporal variability, and diurnal characteristics of the monsoon surface flow using the CSU gridded products. And secondarily, to compare these analyses with those from a special North American Regional Reanalysis for NAME (NARR_NAME), which was produced for the same period. The CSU analyses over the interior land portion of the NAME domain are independent of model data and thus are useful for validating reanalyses and other model products. Compared to the NARR_NAME, the CSU analysis has smaller biases and RMS errors, giving us confidence that it is accurately depicting surface conditions over the NAME domain.

Our major findings are as follows:

- NARR_NAME surface analyses exhibit a cool and dry bias over much of the Mexican mainland. These biases appear to have several ramifications on other model fields. While diagnosing the reasons for these biases in the NARR_NAME is beyond the scope of this study, they are likely related to issues with the land surface model, as well as boundary layer resolution and parameterizations.
- Wind speeds are generally too strong and wind persistence too large in the NARR_NAME. In addition, the nighttime/early morning land breeze at GoC coastal sites is either too weak or missing completely in the NARR_NAME.
- A well-developed land–sea breeze circulation is observed on both sides of the GoC. EOP-mean surface observations from sites along the west Mexican mainland coast show a weak land breeze (0.5–1 m s^{-1}) that peaks near 0900 LT and a daytime sea breeze (~4 m s^{-1}) peaking near 1700 LT. The peaks in these breeze circulations lag the diurnally changing temperature gradient by about 2 h.
- Observations from high elevation sites show near-saturated conditions and low cloud bases during nighttime hours. On the western slopes of the SMO, weak upslope flows (~1 m s^{-1}) are observed during the day, and weak downslope flows (~0.5 m s^{-1}) at night. These observations corroborate the notion of Nesbitt and Gochis (2008) that the presence of high-terrain nocturnal clouds limits radiational cooling and thus nocturnal downslope flows.
- A significant dry bias is seen at the higher elevations of the SMO in the NARR_NAME with slope flows over the higher terrain a factor of 2–3 times stronger than observed. This dry bias may lead to less nighttime cloudiness over the higher terrain and, thus, enhanced radiative cooling in the overnight hours, which would drive stronger nighttime downslope flows. This scenario is consistent with the NARR_NAME's nighttime cool bias at high elevations and with its stronger downslope flows. On the other hand, the lack of nighttime cloudiness in the NARR_NAME could also result in a more rapid warmup of the higher peaks and the stronger daytime upslope flow seen in the NARR_NAME. An alternative explanation for the stronger daytime upslope flow may

be related to its analysis scheme, which is strongly constrained by assimilation of observed precipitation. In this scenario, the NARR_NAME may attempt to compensate for its dry bias by generating a large-scale environment (i.e., stronger upslope flows) conducive to more vigorous convection.

- The daytime transition to surface convergence and rising motion over the western slopes of the SMO occurs about 3 h earlier in the NARR_NAME compared to the CSU analysis. Despite the strong constraints placed on the NARR_NAME by assimilating observed precipitation, these results indicate its tendency to initiate the daily convective cycle too early, similar to that observed in the Eta Model and GFS operational forecast models over this region, which reach their convective maxima ~3 h earlier than observed (Janowiak et al. 2007). Coarse-resolution general circulation models (e.g., NCEP's CDAS) have also shown this tendency to reach their convective maximum 2–3 h too early over this region (Gutzler et al. 2005; Higgins et al. 2000).
- As the monsoon progresses, increased soil moisture, cloud cover, and evapotranspiration due to vegetative green-up result in a weaker diurnal temperature signal over land. In response to this weaker heating cycle, the magnitude and offshore extent of the land–sea breeze circulation is observed to diminish.
- An examination of surface latent and sensible heat fluxes at a land and an oceanic site show that the NARR_NAME substantially overestimates these fluxes (by 42 W m^{-2} at the land site and 69 W m^{-2} at the ocean site). Factors that likely contributed to these higher than observed heat fluxes include differences in flux formulation, the NARR_NAME's surface cool and dry bias, and an excessive downward shortwave radiation (~40 W m^{-2}) in the NARR_NAME.

The foregoing description of surface conditions during the North American monsoon reveals a complexity in the surface flow over a wide range of temporal and spatial scales. Given such conditions, it is hardly surprising that models and reanalysis schemes have difficulty in reproducing these complex features. Hopefully, the analyses presented herein and their comparisons to reanalysis fields have elucidated issues that will lead to improvements in model physics, assimilation schemes, and ultimately to better forecasts of warm season weather.

Acknowledgments. This research has been supported by the National Aeronautics and Space Administration under Grant NNX07AD35G, the National Oceanic and Atmospheric Administration under Grant NA17RJ1228, and under the National Science Foundation under Grants ATM-06639461 and ATM-0340602. We thank Brian McNoldy for providing the QuikSCAT winds; Richard Taft for his assistant with numerous computer and computational issues; Dr. Leslie Hartten for providing the surface flux data for Obispo, Sinaloa; and Ian Baker and Dr. Robert Zamora for several helpful discussions concerning the surface energy budget at the Obispo site. We also appreciate the insightful and careful reviews from Dr. Hugo Berbery and one anonymous reviewer.

REFERENCES

Adams, D. K., and A. C. Comrie, 1997: The North American monsoon. *Bull. Amer. Meteor. Soc.,* **78,** 2197–2213.

Alcantara, A. O., I. Luna, and A. Velaquez, 2002: Altitudinal distribution patterns of Mexican cloud forests based upon preferential characteristic genera. *Plant Ecol.,* **161,** 167–174.

Argote, M. L., A. Amador, M. F. Lavín, and J. R. Hunter, 1995: Tidal dissipation and stratification in the Gulf of California. *J. Geophys. Res.,* **100,** 16 103–16 118.

Badan-Dangon, A., C. E. Dorman, M. A. Merrifield, and C. D. Winant, 1991: The lower atmosphere over the Gulf of California. *J. Geophys. Res.,* **96,** 16 877–16 896.

Berbery, E. H., 2001: Mesoscale moisture analysis of the North American monsoon. *J. Climate,* **14,** 121–137.

Bordoni, S., P. E. Ciesielski, R. H. Johnson, B. D. McNoldy, and B. Stevens, 2004: The low-level circulation of the North American monsoon as revealed by QuikSCAT. *Geophy. Res. Lett.,* **31,** L10109, doi:10.1029/2004GL020009.

Brenner, I. S., 1974: A surge of maritime tropical air—Gulf of California to the southwestern United States. *Mon. Wea. Rev.,* **102,** 375–389.

Douglas, M. W., 1995: The summertime low-level jet over the Gulf of California. *Mon. Wea. Rev.,* **123,** 2334–2347.

——, and J. C. Leal, 2003: Summertime surges over the Gulf of California: Aspects of their climatology, mean structure, evolution from radiosonde, NCEP reanalysis, and rainfall data. *Wea. Forecasting,* **18,** 55–74.

——, J. F. Mejia, J. M. Galvez, R. Orozco, and J. Murillo, 2006: The seasonal evolution of the diurnal variation of the low-level winds around the Gulf of California. Is there a link to vegetation green-up during the wet season? Preprints, *18th Conf. on Climate Variability and Change,* Atlanta, GA, Amer. Meteor. Soc., J3.4. [Available online at http://ams.confex.com/ams/pdfpapers/104717.pdf.]

Fairall, C. W., E. F. Bradley, D. P. Rodgers, J. B. Edson, and G. S. Young, 1996: Bulk parameterization of air-sea fluxes for TOGA-COARE. *J. Geophys. Res.,* **101,** 3747–3767.

Gochis, D. J., A. J. Jimenez, C. J. Watts, J. Garatuza-Payan, and W. J. Shuttleworth, 2004: Analysis of 2002 and 2003 warm-season precipitation from the North American Monsoon Experiment event rain gauge network. *Mon. Wea. Rev.,* **132,** 2938–2953.

——, C. J. Watts, J. Garatuza-Payan, and J. Cesar-Rodriguez, 2007: Spatial and temporal patterns of precipitation intensity as observed by the NAME event rain gauge network from 2002 to 2004. *J. Climate,* **20,** 1734–1750.

Gutzler, D. S., and Coauthors, 2005: The North American Mon-

soon Model Assessment Project: Integrating numerical modeling into a field-based process study. *Bull. Amer. Meteor. Soc.,* **86,** 1423–1430.

Hales, J. E., Jr., 1972: Surges of maritime tropical air northward over the Gulf of California. *Mon. Wea. Rev.,* **100,** 298–306.

Higgins, R. W., W. Shi, E. Yarosh, and R. Joyce, 2000: Improved United States precipitation quality control systems and analysis. *NCEP/Climate Prediction Center Atlas,* No. 7, 47 pp. [Available online at http://www.cpc.ncep.noaa.gov/research_papers/ncep_cpc_atlas/7/index.html.]

——, ——, and C. Hain, 2004: Relationship between Gulf of California moisture surges and precipitation in the southwestern United States. *J. Climate,* **17,** 2983–2997.

Higgins, W., and Coauthors, 2006: The NAME 2004 field campaign and modeling strategy. *Bull. Amer. Meteor. Soc.,* **87,** 79–94.

Huffman, G. J., R. F. Adler, S. Curtis, D. T. Bolvin, and E. J. Nelkin, 2007: Global rainfall analyses at monthly and 3-hr time scales. *Measuring Precipitation from Space: EURAINSAT and the Future,* V. Levizzani, P. Bauer, and J. Turk, Eds., Kluwer Academic, 291–306.

Janowiak, J. J., V. J. Dagostaro, and R. J. Joyce, 2007: An examination of precipitation in observations and model forecasts during NAME with emphasis on the diurnal cycle. *J. Climate,* **20,** 1680–1692.

Johnson, R. H., P. E. Ciesielski, B. D. McNoldy, P. J. Rogers, and R. K. Taft, 2007: Multiscale variability of the flow during the North American Monsoon Experiment. *J. Climate,* **20,** 1628–1648.

Joyce, R. J., J. E. Janowiak, P. A. Arkin, and P. Xie, 2004: CMORPH: A method that produces global precipitation estimates from passive microwave and infrared data at high spatial and temporal resolution. *J. Hydrometeor.,* **5,** 487–503.

Lang, T. L., D. A. Ahijevch, S. W. Nesbitt, R. E. Carbone, S. A. Rutledge, and R. Cifelli, 2007: Radar-observed characteristics of precipitating systems during NAME 2004. *J. Climate,* **20,** 1713–1733.

Lavín, M. F., and S. Organista, 1988: Surface heat flux in the northern Gulf of California. *J. Geophys. Res.,* **93,** 14 033–14 038.

——, R. Durazo, E. Palacios, M. L. Argote, and L. Carrillo, 1997: Lagrangian observations of the circulation in the northern Gulf of California. *J. Phys. Oceanogr.,* **27,** 2298–2305.

Lin, Y., K. E. Mitchell, E. Rogers, M. E. Baldwin, and G. J. DiMego, 1999: Test assimilations of the realtime, multisensor hourly precipitation analysis into the NCEP Eta Model. Preprints, *Eighth Conf. on Mesoscale Meteorology,* Boulder, CO, Amer. Meteor. Soc., 341–344.

Liu, W. T., 2002: Progress in scatterometer applications. *J. Oceanogr.,* **58,** 121–136.

Luo, H., and M. Yanai, 1983: The large-scale circulation and heat sources over the Tibetan Plateau and surrounding areas during the early summer of 1979. Part I: Precipitation and kinematic analysis. *Mon. Wea. Rev.,* **111,** 922–944.

Mahrer, Y., and R. A. Pielke, 1977: The effects of topography on sea and land breezes in a two-dimensional model. *Mon. Wea. Rev.,* **105,** 1151–1161.

McNoldy, B. D., P. E. Ciesielski, and R. H. Johnson, 2006: Diurnal cycle of sea surface winds and temperatures during the 2004 North American Monsoon Experiment. Preprints, *27th Conf. on Hurricanes and Tropical Meteorology,* Monterey, CA, Amer. Meteor. Soc., P2.2. [Available online at http://ams.confex.com/ams/pdfpapers/108534.pdf.]

Mesinger, F., and Coauthors, 2006: North American Regional Reanalysis. *Bull. Amer. Meteor. Soc.,* **87,** 343–360.

Mo, K. C., E. Rogers, W. Ebisuzaki, R. W. Higgins, J. Woollen, and M. L. Carrera, 2007: Influence of the North American Monsoon Experiment (NAME) 2004 enhanced soundings on NCEP operational analyses. *J. Climate,* **20,** 1821–1842.

Nesbitt, S. W., and D. J. Gochis, 2008: The diurnal cycle of clouds and precipitation along the Sierra Madre Occidental observed during NAME-2004: Implications for warm season precipitation estimation in complex terrain. *J. Hydrometeor.,* in press.

Nuss, W. A., and D. W. Titley, 1994: Use of multiquadric interpolation for meteorological objective analysis. *Mon. Wea. Rev.,* **122,** 1611–1631.

Paden, C. A., M. R. Abbott, and C. D. Winant, 1991: Tidal and atmospheric forcing of the upper ocean in the Gulf of California. Part I: Sea surface temperature variability. *J. Geophys. Res.,* **96,** 18 337–18 359.

Reiter, E. R., and M. Tang, 1984: Plateau effects on diurnal circulation patterns. *Mon. Wea. Rev.,* **112,** 638–651.

Rogers, P. J., and R. H. Johnson, 2007: Analysis of the 13–14 July Gulf surge event during the 2004 North American Monsoon Experiment. *Mon. Wea. Rev.,* **135,** 3098–3117.

Sardeshmukh, P., and B. J. Hoskins, 1984: Spatial smoothing on the sphere. *Mon. Wea. Rev.,* **112,** 2524–2529.

Stull, R. B., 1995: *Meteorology Today: For Scientist and Engineers.* West Publishing, 385 pp.

Wang, W., and P. Xie, 2007: A multiplatform-merged (MPM) SST analysis. *J. Climate,* **20,** 1662–1679.

Watts, C. J., R. L. Scott, J. Garatuza-Payan, J. C. Rodriguez, J. H. Prueger, W. P. Kustas, and M. Douglas, 2007: Changes in vegetation condition and the surface fluxes during NAME 2004. *J. Climate,* **20,** 1810–1820.

Wexler, R., 1946: Theory and observations for land and seabreezes. *Bull. Amer. Meteor. Soc.,* **27,** 272–287.

Xie, P., Y. Yarosh, M. Chen, R. Joyce, J. J. Janowiak, and P. A. Arkin, 2005: Diurnal cycle of cloud and precipitation associated with the North America Monsoon System: Preliminary results for 2003 and 2004. Preprints, *16th Conf. on Climate Variability and Change,* San Diego, CA, Amer. Meteor. Soc., 4.22. [Available online at http://ams.confex.com/ams/pdfpapers/82939.pdf.]

Zhu, C., T. Cavazos, and D. P. Lettenmaier, 2007: Role of antecedent land surface conditions in warm season precipitation over northwestern Mexico. *J. Climate,* **20,** 1774–1791.

Zuidema, P., C. Fairall, L. M. Hartten, J. E. Hare, and D. Wolfe, 2007: On the air–sea interaction at the mouth of the Gulf of California. *J. Climate,* **20,** 1649–1661.